ANALYSIS OF THE THERMAL-HYDRAULIC RESPONSE OF THE REACTOR CAVITY COOLING SYSTEM DURING ACCIDENT SCENARIOS USING THE RELAP5/SCDAPSIM SYSTEM CODE

A Thesis

by

HATICE NUR UNVER

Submitted to the Graduate and Professional School of
Texas A&M University
in partial fulfillment of the requirements for the degree of

MASTER OF SCIENCE

Chair of Committee,	Yassin A. Hassan
Committee Members,	Rodolfo Vaghetto
	Victor Ugaz
Head of Department,	Michael Nastasi

August 2021

Major Subject: Nuclear Engineering

ABSTRACT

The Reactor Cavity Cooling System (RCCS) is one of the passive safety systems included in the design of Generation IV reactors. The RCCS is designed to remove the heat from the reactor cavity by natural circulation without any human intervention, during normal operations and accident conditions. In this study, a model representing the Texas A&M University 1/23 scaled water-cooled RCCS experimental facility has been prepared using the RELAP5/SCDAPSIM system code. Simulations of steady-state configurations have been performed and compared with the available experimental data to validate the models. Transient simulations were performed to study the thermal-hydraulic behavior of the RCCS under hypothetical accident conditions involving the blockage of selected risers. The results of the simulations provided additional information on the behavior of the RCCS during those accidents.

DEDICATION

To my family for their invaluable love and support.

ACKNOWLEDGEMENTS

I would like to first thank Dr. Yassin A. Hassan for providing me the opportunity for this research and my committee members, Dr. Rodolfo Vaghetto, and Dr. Victor Ugaz, for their guidance and support throughout the course of this research. Special thanks to Alessandro Vanni for his guidance and sincere help with this research. Thanks to Dr. Chris Allison and Innovative Systems Software for providing the software license and supports for this project.

Thanks also go to my friends and colleagues and the department faculty and staff for making my time at Texas A&M University a great experience.

Finally, thanks to my mother and father for their everlasting support and prayers.

CONTRIBUTORS AND FUNDING SOURCES

Contributors

This work was supervised by a thesis committee consisting of Dr. Yassin A. Hassan and Dr. Rodolfo Vaghetto of the Department of Nuclear Engineering and Dr. Victor Ugaz of the Department of Chemical Engineering.

The data which is analyzed in Chapter 2 was provided by Dr. Hassan.

Funding Sources

Graduate study was supported by a scholarship from Republic of Turkey Ministry of National Education.

TABLE OF CONTENTS

Page

LIST OF FIGURES

FIGURE Page

LIST OF TABLES

TABLE Page

1. INTRODUCTION

Nuclear reactors are one of the important energy sources that can contribute to the reduction of CO_2 emissions. Improved energy resources are needed to protect the world from greenhouse gasses that play a significant role in climate change. In line with the increasing world population and energy demanding needs, new-generation nuclear reactor designs have been proposed, following the technology development of Gen I, II, III, III+, and IV.

Generation I reactors were designed as power and prototype reactors in the 1950s and 1960s. Generation II reactor systems were designed in the 1960s to be more economical and reliable than Generation I. Pressurized water reactors (PWR), boiling water reactors (BWR), Canada Deuterium Uranium reactors (CANDU), Vodo-Vodyanoi Energetichesky reactors (VVER), and advanced gas-cooled reactors (AGR) are Generation II reactor systems.

Generation III nuclear reactors are Generation II reactors with improved, design technology innovations in terms of safety, thermal efficiency, fuel technology, and design. Passive safety systems are used in this generation and they have been planned for about 60 years of operational lifetime. Advanced PWR (AP-600), advanced boiling water reactor (ABWR), enhanced CANDU 6, and System 80+ are Generation III reactor systems. Generation III + are the reactor type with advanced safety improvements of Generation III. VVER-1200/392M, Advanced CANDU Reactor (ACR-1000), Advanced PWR (AP-1000), European Pressurized Reactor (EPR), and Economic Simplified Boiling Water Reactor (ESBWR) are types of Generation III + reactors.

The next generation of reactors, Generation IV reactors have essential developments in terms of safety and reliability, economics, and sustainability of energy. Generation IV reactors consist of six different technological reactor systems: the very-high-temperature reactor (VHTR), the gas-cooled fast reactor (GFR), the lead-cooled fast reactor (LFR), the molten salt-cooled reactor (MSR), the sodium-cooled fast reactor (SFR), and the supercritical water-cooled reactor (SCWR) [1], [2]. New passive safety systems have been integrated into the Gen-IV reactors. Reactor Cavity Cooling Systems (RCCSs) are one of the passive safety systems and are used in generation IV reactors, even if it was initially designed for the High Temperature Gas Cooled Reactor (HTGR).

For this study,

- A RELAP/SCDAPSIM simulation model for the TAMU RCCS experimental facility was built in RELAP5/SCDAPSIM system code and validated for normal operation conditions against steady-state experimental data.
- Simulations of the facility response to the one riser blockage and loss of cooling system accidents conditions were performed and analyzed.

This chapter provides some background of the VHTR and RCCS designs, the previous studies on the RCCS that are available in literature, and the objectives of the study.

In the second chapter, a description of the experimental facility main features and components along with the geometrical and experimental data that were used to build our simulation model are provided.

In the next chapter, the RELAP5/SCDAPSIM system code and the simulation models are described. For this study three models were built: the steady-state model, the single riser blockage accident transient model, and the loss of the cooling system accident model.

In chapter 4, the steady-state simulation results are compared with experimental data for validation purposes. The single riser blockage accident simulation results are analyzed and the loss of cooling system condition simulation results are compared to experimental data, this time not for validation purposes but to evaluate the performance of the model under these conditions.

1.1 The Reactor Cavity Cooling Systems (RCCS) for VHTR

The next generation gas-cooled Very High Temperature Reactor (VHTR) that uses graphite moderators and helium coolant could operate at a very high exit temperature (900-1300K according to El-Genk and Tournier (2017)) The rise in the exit temperature will increase thermal efficiency to generate electricity. Therefore, passive safety systems capable to dispose of the heat without any human intervention or active component, have been adopted into these reactors to increase safety [3],[4].

The passive safety systems for nuclear reactors have an important role to prevent the plant from evolving into non-safe conditions. After the Fukushima Daiichi Reactor accident in 2011 [5], the passive safety systems gained more importance and they have been improved [6]. The RCCS is a passive safety systems capable of disposing the heat produced in the reactor pressure vessel (RPV) throughout natural circulation without any human intervention. During both normal operations and accident conditions, even when the power is lost, the RCCS can keep the temperature in the vessel and in other containment materials within their safety margins and

to guarantee the necessary high level of safety. RCCS has two type designs that depend on the water-cooled and air-cooled. In this study, a water-cooled RCCS was considered during the simulations [7].

1.2 Literature Review

The passive nuclear safety systems have been an important study and they are widely studied in nuclear science. A 1/23 scaled water-cooled RCCS experimental facility was designed and constructed at TAMU experimental facility to investigate thermal hydraulic phenomena during both steady-state and transient conditions. The previous study indicated the design and investigation of the used experimental facility[8]. The thermal-hydraulic behavior of the experimental facility applications with model development and validations using the system codes RELAP5-3D and CFD were studied [9], [10]. Additionally, various studies in the same experimental facility have investigated the flow distribution of natural circulation inside the multi-branch manifold, and the wall temperatures with distributed fiber optic sensors [11], [12].

The loss of one of the risers of the facility is one of the hypothetical accidents that could occur in an RCCS, jeopardize the main safety feature, and reduce the heat removing capabilities [13].

Experimental studies have been performed to evaluate the responses of the University of Wisconsin water cooled RCCS experimental facility to investigate two-phase flow natural circulation. Based on the experimental result, the two-phase natural circulation showed transition flow under the performed accident conditions and flow transition instabilities were observed [14]. Under those conditions, the creation of a void in the system led to flow instabilities and vibrations which can impact the structural stability and the heat transfer [15].

Vaghetto et al. (2020) analyzed the two-phase natural circulation flow measurement and observations in the 1/23 scaled water-cooled TAMU RCCS experimental facility [16]. Once the system reached the steady-state condition, the cooling system was shut down to observe two-phase flow. The high-resolution measurement data was obtained during the transient condition. The system results were shown during subcooled conditions, the flow showed a stable, symmetric distribution through the risers, and the void fraction was lower than 0.3 for all risers. When the temperature reached saturation value, flow instabilities, the void fractions about 0.9 and flow stagnation, and inversions were observed.

1.3 The Purpose of the Study

This study aimed to investigate the simulation of the thermal-hydraulic behavior of the TAMU RCCS facility during single-riser blockage and loss of the cooling system accidents conditions by using the thermal-hydraulic RELAP5/SCDAPSIM system code. Loss of the riser and loss of the cooling system accidents are possible to observe in RCCS. Since the experiments are expensive and time consuming, we built a simulation model with the thermal-hydraulic system code of RELAP5/SCDAPSIM based on the Texas A&M University RCCS experimental facility to provide additional data. The model validated against the available steady-state experimental data, as described in Chapter III, and the model can be used also to design additional experiment in the facility. Such steady-state model, was then used to simulate the evolution of the TAMU RCCS experimental facility under the single riser blockage accident conditions. The simulation results of this case were analyzed in paragraph 4.2.

The analysis of the loss of the cooling system in the TAMU RCCS experimental facility was presented in 4.3. A simulation model was built for this study and the results were compared

with experimental data from the same facility in analogous conditions. The single-phase flow and two-phase flow instabilities of the simulation were investigated. The simulated response of the RCCS facility was used to infer the response of the scaled TAMU RCCS under the same conditions, the possible degradation of the safety function of the RCCS. The simulations were used to improve the understanding of the TAMU RCCS experimental facility, as it allowed us to infer quantities not measured during the experiments but could be inferred based on the simulation results.

2. THE RCCS EXPERIMENTAL FACILITY AND AVAILABLE DATA

In this study, the scaled-down water-cooled RCCS experimental facility was studied and all simulated research models were based on the RCCS, which is located in Texas A&M University at the Thermal-Hydraulic Research Laboratory of the Department of Nuclear Engineering.

The RCCS facility is a 1:23 axial length scale with a single risers' cooling panel. The cooling panel with a compound of 9 riser pipes and fins in the cavity section, the risers were connected with lower and upper manifolds. The components of the facility are three electrical radiant heaters, which represent the reactor vessel, one risers' cooling panel which is composed of nine riser pipes that are connected with lower and upper manifolds, the water tank with its connecting pipes, and the chiller with its connecting pipes. The risers are assembled with fins which are thin metal panels to increase the radiation heat transfer. The upper manifold is connecting to a cylindrical water tank with pipes that are called hot legs. The cylindrical water tank is located at the top of the cavity region. The tank is connected to the lower manifold with pipes that are called cold legs from the tank's bottom side to the lower manifold [10]. The components of the facility are shown in Figure 1.

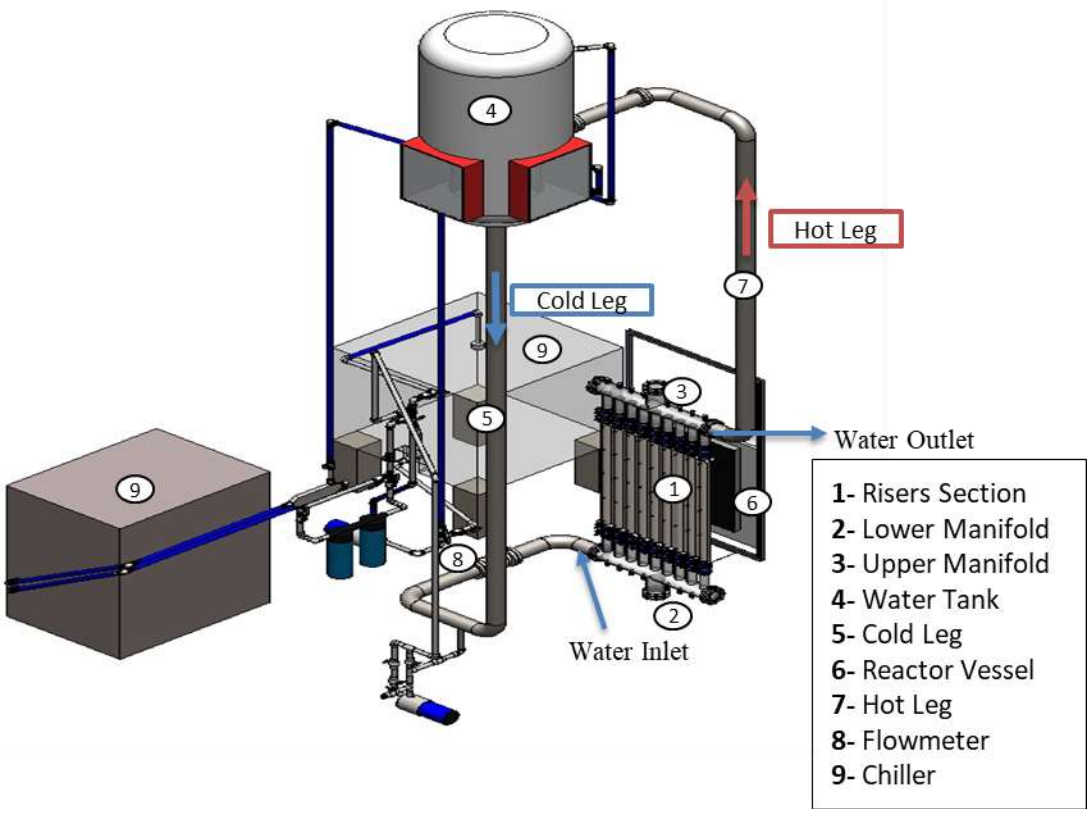

Figure 1. The experimental system components

In the system, the electrical radiant heaters in the reactor vessel provide heat to the system. The heaters are represented as the heat source and water tank are represented as the heat sink for this system. During the normal operation (steady-state) experiment, heat is generated by the three electrical radiant heaters and is transferred by radiation and natural convection heat transfers to the RCCS cooling water and fins. The fins transfer the gathered heat to risers' walls by conduction, then the heat is transferred to the coolant by convection. When the cooling water gets warmed up, the buoyancy forces generate induces natural circulation in the system. The heated water moves upward inside the risers toward the upper manifold and the water tank. Over there, the heat is removed by mixing the water of the primary loop with the water coming from the chiller. The colder water flows from the bottom of the tank and flows downward toward the lower manifold, then enters through the risers from the bottom and closes the loop [8].

The available experimental data generated during steady-state tests at the facility are:

- the total volumetric flow rate of the system,
- the risers' coolant temperatures at five different elevations,
- the coolant temperatures at the inlet and outlet of the cooling panel,
- tank inlet and outlet temperatures

In the facility, thermocouples are installed to measure the temperature inside each riser at five different elevations. The total volumetric flow rate in the primary loop is measured and recorded by a flow meter installed upstream of the lower manifold, as shown in Figure 2[9].

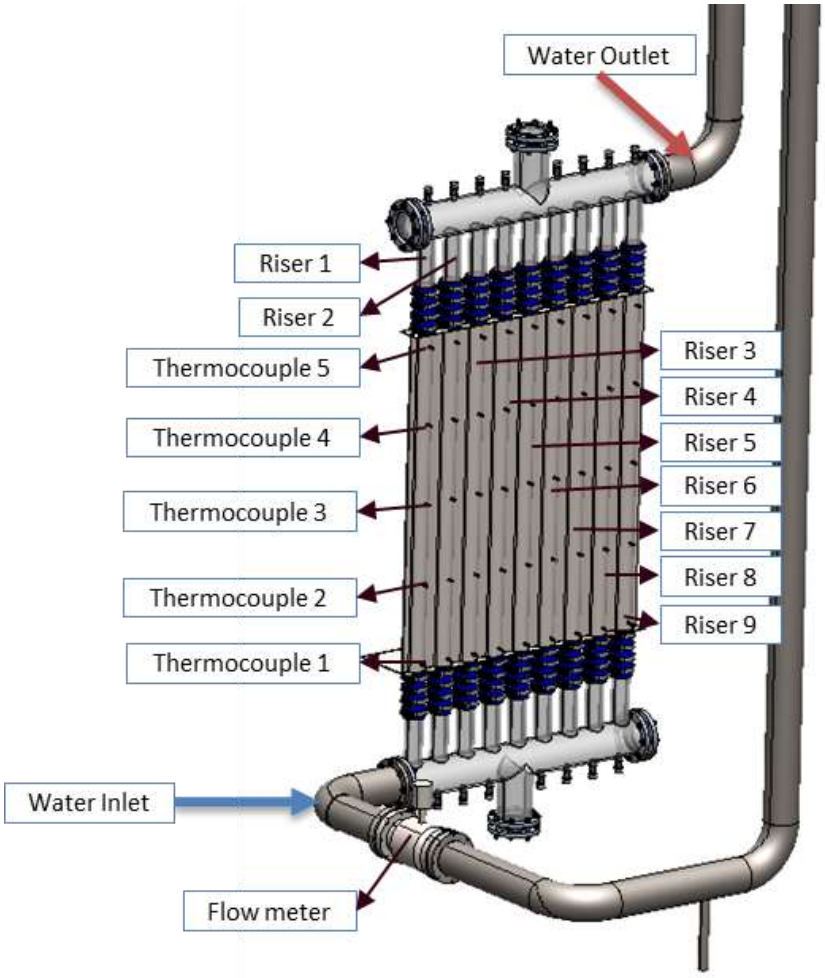

Figure 2. View of the nine riser pipes with the locations of the thermocouples showed

The total pressure drop within the main loop can be adjusted with a butterfly valve that is located at the exit of the tank. For this study, two experimental data sets were used corresponding to two different valve opening conditions (25% and 100% open), at steady-state operating conditions. The first condition (25% opening area) is the one providing the highest pressure drop with subsequent lowest loop flow rate. The fully opened valve conditions (100%) resulted in the lowest loop pressure drop, and subsequent highest loop flow rate.

Experimental data was provided for normal operation (steady state) conditions that were used to validate the simulation model. In this study, we investigated two cases; the valve is 25% open and 100% open for normal operation conditions concerning the experimental data. The facility total system volumetric flow rate in these two conditions is listed in Table 1 for both cases.

Table 1. The experimental results of the system total volumetric flow rates

Case	Volumetric Flow Rate (LPM)
Valve 25% Open	8.2 ± 0.3
Valve 100% Open	39 ± 0.6

The experimental data of the water temperatures through thermocouple locations inside the risers are shown in Figure 3 and Figure 4 respectively for the case valve 25% open and valve 100% open.

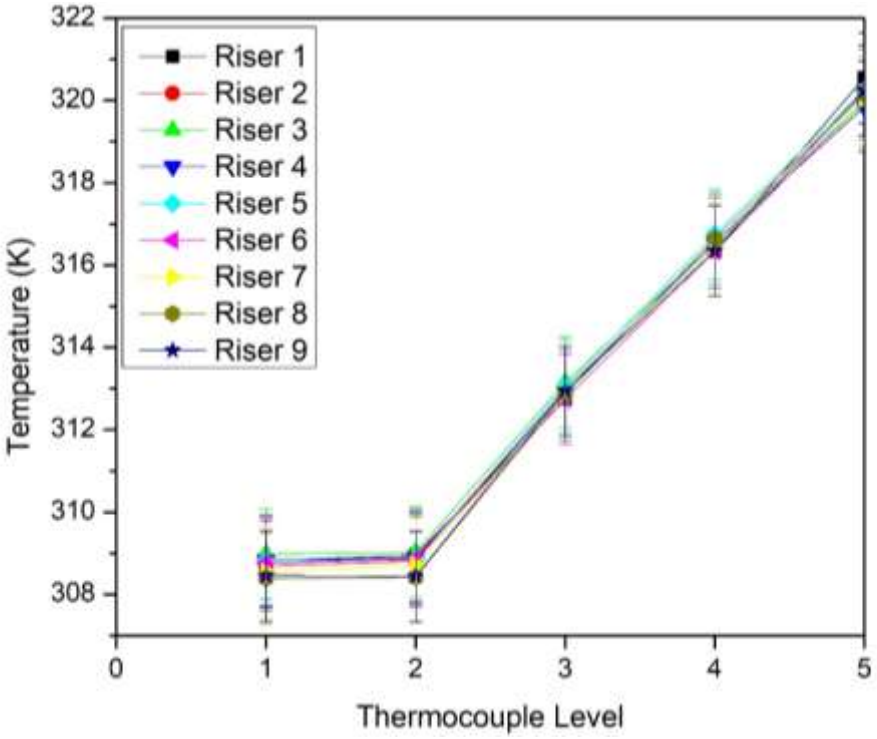

Figure 3. The experimental results of the thermocouple temperatures for the valve 25% open.

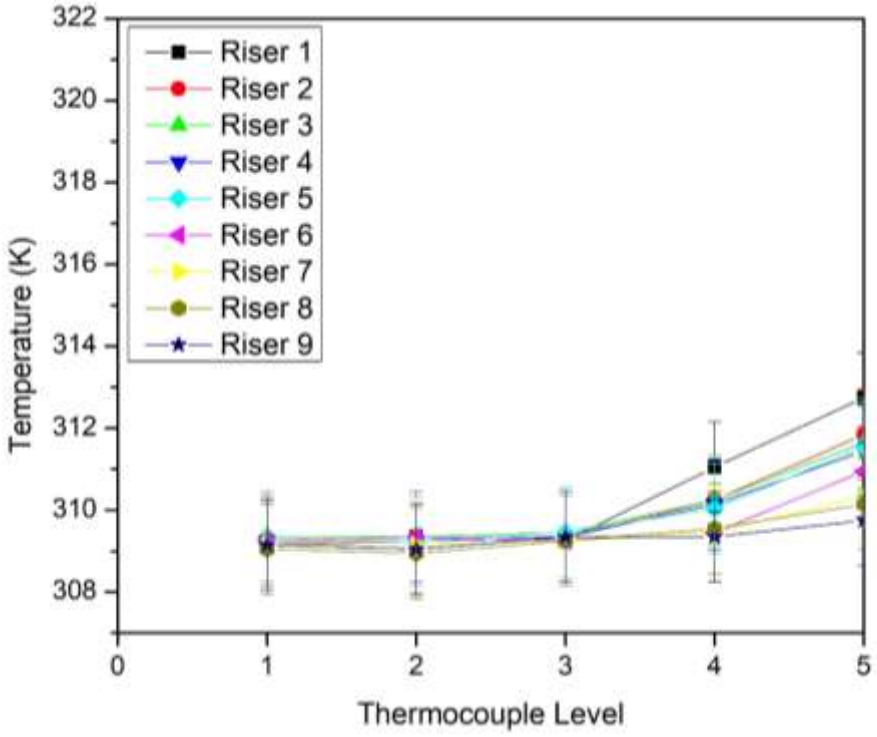

Figure 4. The experimental results of the thermocouple temperatures for the valve 100% open.

By using Equation 1, the total mass flow rates of the systems were calculated for both cases. The densities in the equation were used according to the cavity inlet temperature values.

$$\dot{m} = \rho \cdot \dot{V} \qquad \text{Equation 1.}$$

where ;

$\dot{m}$= mass flow rate (kg/s),

$\rho = density\ (kg/\mathrm{m}^3)$,

$\dot{V}$= volumetric flow rate (LPM)

The experimental data of the system cavity inlet and cavity outlet temperatures, and the calculated system total mass flow rates for both cases are shown in **Error! Reference source not found.**.

Table 2. The cavity temperatures and calculated mass flow rates.

	Valve 25% Open	Valve 100% Open
Mass Flow Rate (Kg/s)	0.1358 ± 0.05	0.646 ± 0.01
Cavity Inlet Temperature (K)	308.99 ± 0.2	309.29 ± 0.2
Cavity Outlet Temperature (K)	321.59 ± 0.2	312.09 ± 0.2

By using Table 2 data and Equation 2, the powers that are given to the systems were calculated. The specific heat of the system is used at the average temperature of the cavity inlet and outlet temperatures.

$$\text{Power} = \dot{m} \cdot C_p \cdot \Delta T \qquad \text{Equation 2.}$$

The calculated powers are 7153.12 ± 286.8 Watts for valve 25% open and 7555.56 ± 551.4 Watts for valve 100% open.

where; $\text{Power} = \dot{m} \cdot C_p \cdot \Delta T$

$\dot{m}$= mass flow rate (kg/s),

C_p = is the specific heat (J/kg*K),

ΔT = is the temperature difference (K)

By considering the above information in model valve 25% and 100 % open cases related to the system flow rate, the RELAP5/SCDAPSIM input decks were built for the normal operation conditions.

3. RELAP5/SCDAPSIM SYSTEM CODE AND SIMULATION MODELS

3.1 RELAP5/SCDAPSIM System Code

The RELAP5/SCDAPSIM system simulation code is designed for reactor system behavior prediction for both normal operation and accident conditions. The RELAP5/SCDAPSIM thermal hydraulic system code is developed and supported by Innovative System Software (ISS) and relies on the models that were developed by the US Nuclear Regulatory Commission (US-NRC) for RELAP/MOD3.3 and SCDAP/RELAP5/MOD3.2 [17]. The RELAP5/SCDAPSIM combines such publicly available models with proprietary advanced programming and numerical methods, user options, and additional methods developed by ISS and other members of the SCDAP Development and Training Program (SDTP) [18].

RELAP5/SCDAPSIM code has been extensively used for a variety of applications. The code is divided into three major versions based on their applications. These applications include the analyses of research reactors, the analysis and design of experiments, the support of the development of improved models, and analytic capabilities. The production versions of RELAP/SCDAPSIM/MOD3.2 and MOD3.4 are used by the licensed user and program members for nuclear power plant and research reactors' critical calculation applications. The most advanced production version of the code is MOD3.4 that is used for the general training of the code; also the experiments of severe accidents can be designed and analyzed in this version. To improve the code accuracy, the advanced modeling options are developed in version MOD4.0 that is available to only program members.

The code is the combination of RELAP5 and SCDAP codes. The thermal hydraulic of the system reactor coolant, reactor kinetics, control system, and noncondensable gases transport of the simulations are analyzed with the part of the code RELAP5 (Reactor Excursion and Leak Analysis Program) and the core structure damage and the reactor vessel lower head analysis models are available in SCDAP (Severe Core Damage Analysis Package) [19].

The RELAP5/SCDAPSIM thermal hydraulic system code predicts the system behavior during both normal and accidental situations. Therefore, the RELAP5/SCDAPSIM thermal hydraulic system code was used to build simulation models' input files and run accident scenarios in this study. The version of RELAP5/SCDAPSIM which was used for this study is RELAP5/SCDAP 3.4.

3.2 Normal Operation RELAP5/SCDAPSIM Simulation Model

A RELAP5/SCDAPSIM model of the scaled water-cooled RCCS experimental facility described in Chapter 2 has been prepared based on geometrical information of the experimental facility. The nodalization diagram of the model of the water-cooled RCCS experimental facility is shown in Figure 5.

In the nodalization diagram, pipe (255) represents the lower manifold component divided into 9 sub-volumes located at the bottom of the riser section. Each sub-volume of the lower manifold is connected to the inlet of the nine riser pipes with single junctions (from 191 to 199). Each of the nine riser pipes (from 201 to 209) are divided into 7 sub-volumes, and they are connected from their outlets to the upper manifold via single junctions (from 211 to 219). The upper manifold (225) is divided into nine sub-volumes, and each sub-volume correlates with a riser.

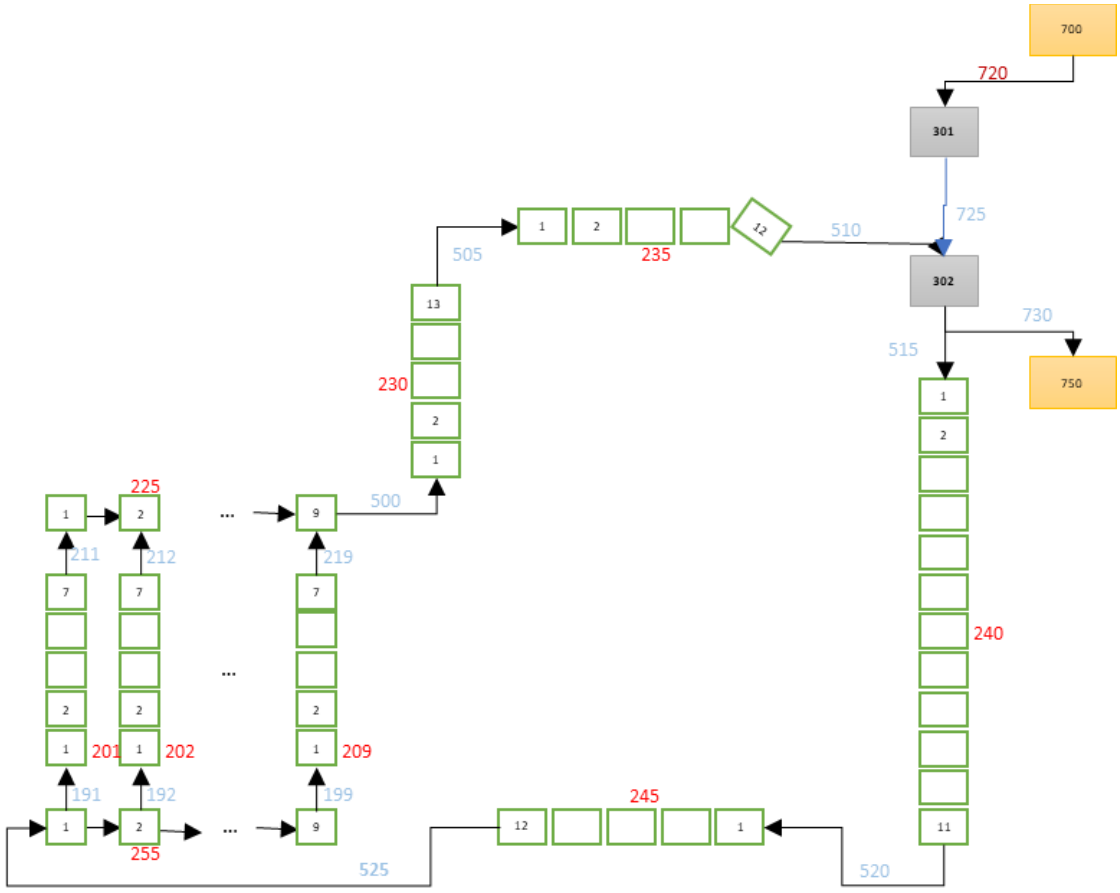

Figure 5. The nodalization diagram of the normal operation simulation.

The upper manifold is connected with a single junction (500) to a pipe (230), representing the vertical portion of the hot leg. The pipe 230 is connected to pipe 235 (the horizontal part of the hot leg) via single junction 505. The horizontal hot leg (pipe 235) discharges water into the tank (302) through a single junction (510). The tank is divided into two single volumes (301 and 302) that are split as shown in Figure 6, based on the water level in the tank and the elevation on the inlet nozzle. The hot water heated in the risers coming through hot leg riser is mixed with cold in the water tank. The mixed cold water in the bottom part of the tank 302 flows downward through the vertical pipe 240 and the horizontal pipe (245), which

represents the cold leg of the facility. The water finally flows back to the lower manifold. The butterfly valve located at the bottom of the water tank in the experimental facility that was simulated by changing the flow area of the corresponding place in the simulation. The K-loss coefficient was calculated based on the valve information provided by the manufacturer, in relation to the valve opening position. The power coefficients were added to the simulation based on the experimental data, but the simulation results were not matched with experimental results. Thus, the friction losses, power, and heat sink parameter were adjusted by trying to validate simulation results with experimental data.

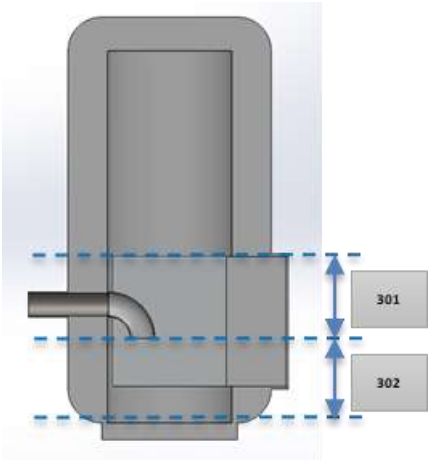

Figure 6. The view of the tank

The time-dependent volumes 700 and 750 define the boundary conditions of the secondary loop. The time-dependent volume 700 is connected with the top of the single volume 301 via a time-dependent junction 720. The boundary conditions were specified as atmospheric pressure and temperature by the time-dependent volume.

In the experiment facility, each riser has five thermocouples to measure the temperatures; in the simulation model, each riser is divided into seven sub-volumes, and the centers of these sub-volumes (from 2 to 6) are positioned at the corresponding elevations of the thermocouples, as shown in Figure 7.

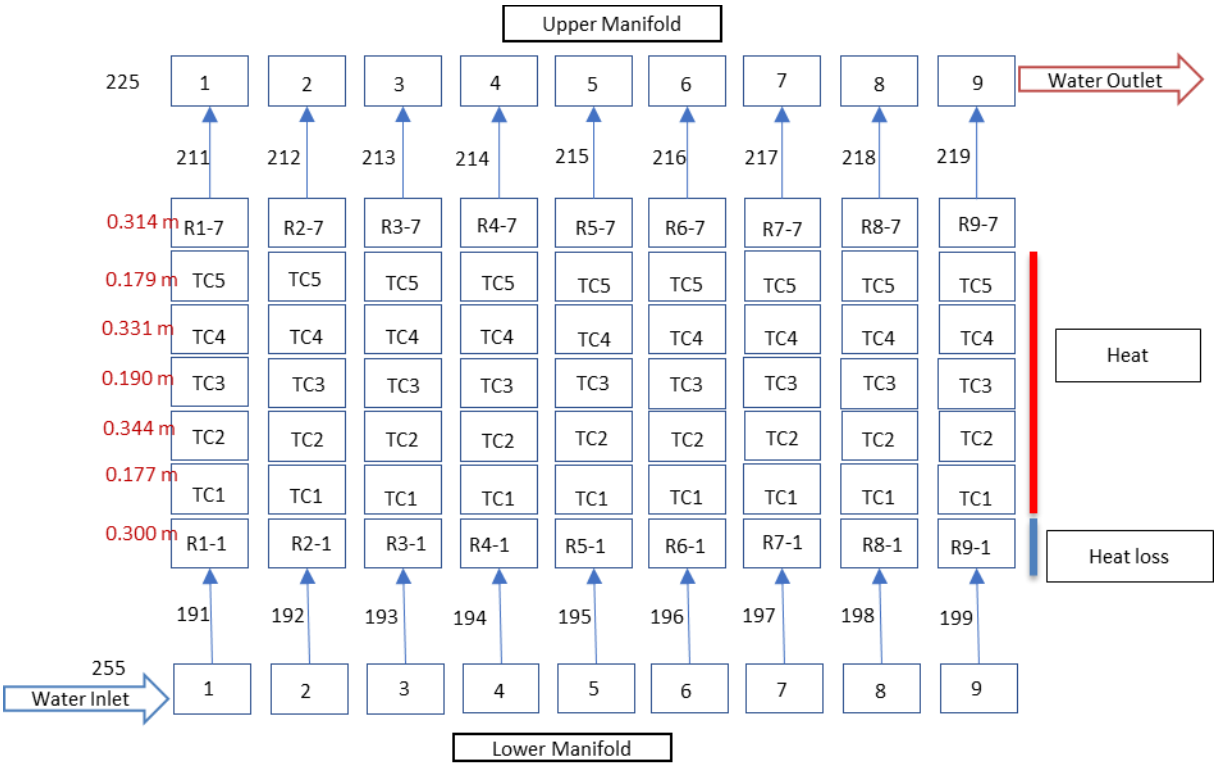

Figure 7. The risers' and thermocouples.

In the facility, the lower part and the upper part of all of the risers are made out of glass for measurement purposes (see Figure 8). In Figure 7, the vertical red line on the right side of the risers highlights the region of the risers where the heat was provided, while the blue line highlights the region of the risers where the heat losses were applied. These parts did not directly face the heating panels of the facility and tended to have significant heat losses; in fact, the water temperatures measured by the lowest level of the thermocouples of the risers were lower in value than the water temperature measured at the cavity inlet. In the simulation model, the heat was produced within heat structures (between 2010 to 2090) directly connected with the risers' components, while the heat losses were modelled through a radiation type of enclosure between the heat structures connected with the bottom part of the risers and a dump heat structure that represents the surrounding environment.

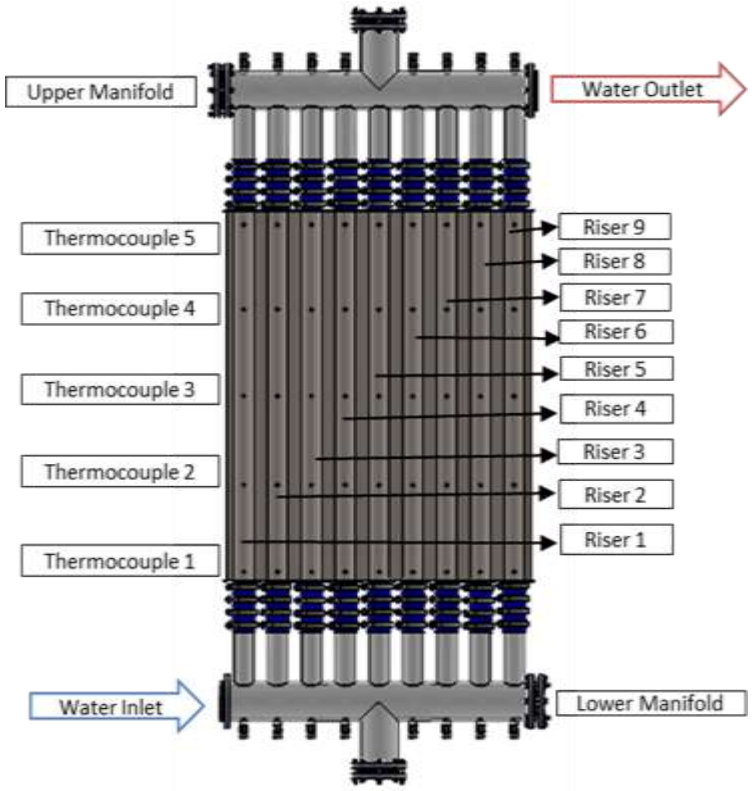

Figure 8. The risers, thermocouples and heat and heat losses are shown.

3.3 Riser Blockage Accident Model

The loss of one of the risers of the facility is one of the hypothetical accidents that could occur in an RCCS. The one riser pipe loss accident was simulated for this study by blocking the water from flowing through one of the risers. In this study, the single riser accident was performed for two cases; the valve is 25% open and 100% open, and both simulation results were investigated.

For the sake of this study, we assumed that the riser number 4 (non-peripherical) gets blocked instantly, while the facility is operating in normal conditions. From the simulation model point of view, the blockage was modelled by the closure of a trip valve at the riser inlet, as shown in Figure 9, where the red sign in the single junction 194 represents the location of the blockage.

Figure 9. The figure shows the riser section and trip valve that is blocked for the one riser loss accident.

As the system reaches steady-state condition after 8000 seconds, the trip valve closing time was set at 8000 seconds. The total simulation time was set at 48000 seconds to observe and analyze the RCCS response during the accident condition.

3.4 Loss of the Cooling System Accident Model

The loss of the active cooling system for the experimental facility was simulated, and the behavior of the fluid and two-phase flow instabilities were analyzed in this study. In this model, the simulation started under normal operation when the system reached steady-state conditions, the cooling system of the model was shut down to obtain transient flow. At the simulation initiative, the case was the valve 100% open, and the provided total power was 7866.3 W to the system during the simulation. Under these conditions, the coolant inside the primary system

eventually reached saturation conditions, and flow instabilities rose. The nodalization diagram of the simulation loss of cooling system model is shown in Figure 10.

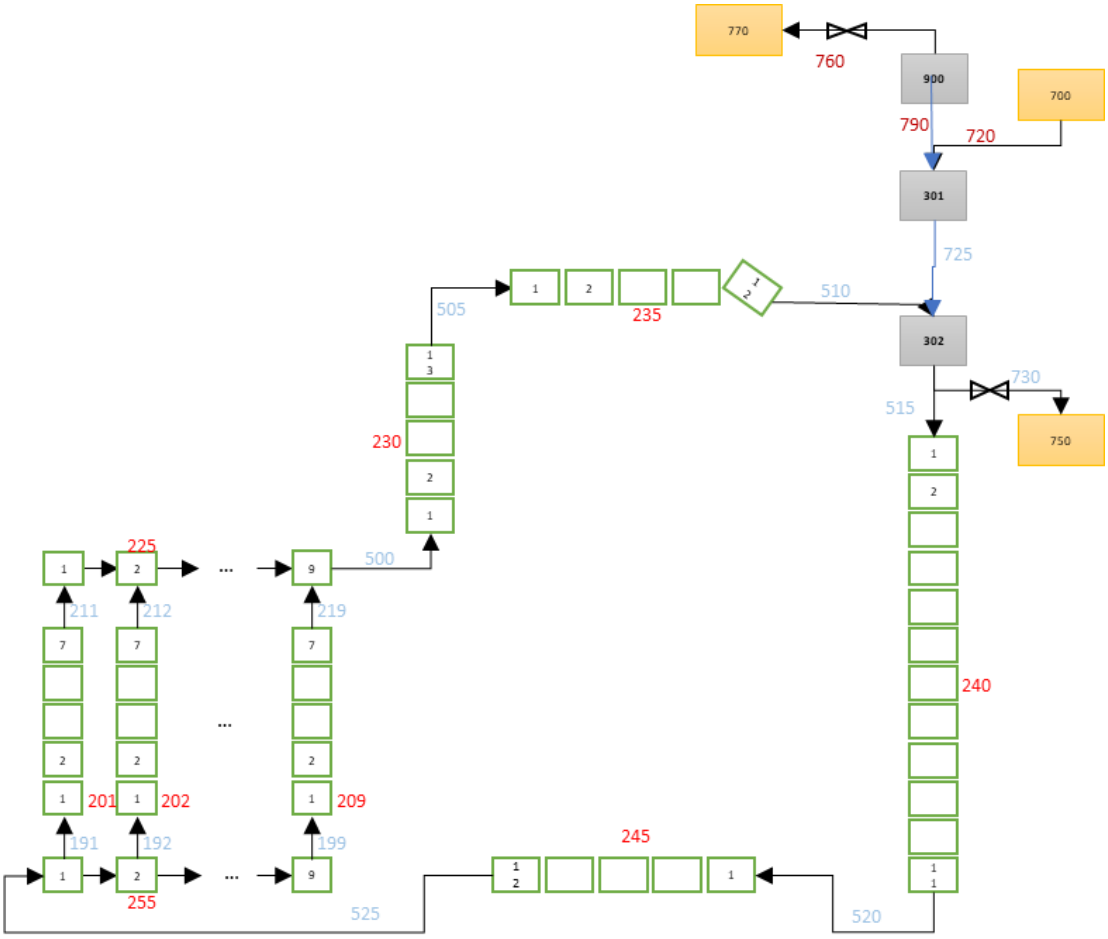

Figure 10. The figure shows the nodalization diagram of the loss of cooling system accident simulation.

Compared to the nodalization diagram of the steady state case (**Error! Reference source not found.**), single volume 900, two trip valves (730 and 760), and time dependent volume 770 were added. The components 700, 750 and 770 are time-dependent junctions. The time dependent junctions 700 and 750 represented the chillers in the experimental facility and they were boundary condition of the simulation. The time-dependent junction 770 was added to the system to adjust atmospheric pressure. Figure 11 shows how the water tank volume was split

between the single volumes 301, 302 and 900. The single volume 900 represents the part of the water tank that is not filled with water during steady state operations.

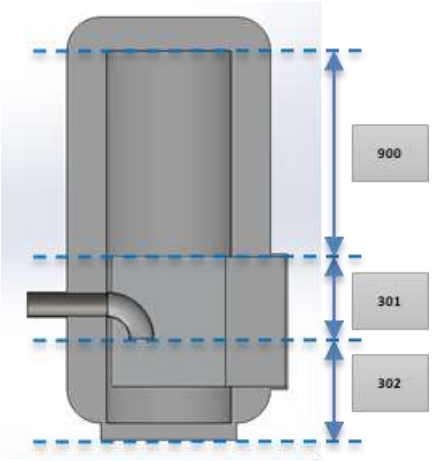

Figure 11. The figure shows the tank of the loss of cooling system accident model.

About 40000 seconds into the scenario was simulated, plus an additional 8000 seconds at the beginning to reach steady state conditions. During this time, the cold water is injected into the tank through the time dependent junction 720 and the same mass flow rate is discharged through the valve 730. After 8000 seconds into the simulation, time dependent junction 720 and valve 730 are switched off, while valve 760 opens up to anchor the pressure of the system to the environment.

4. RESULTS AND DISCUSSION

4.1 Normal Operation Model Simulation Results

In this section, the steady-state models were simulated for the two cases and the system temperatures in the risers and the total system volumetric flow rates were compared to validate the simulation. The comparison results of the RELAP5/SCDAPSIM models under normal operation conditions showed good agreement with the experimental data.

4.1.1 Normal Operation Results Case Valve 25% Open

As described above, five thermocouples at five different levels were placed inside each riser in the experimental facility. In Figure 12, the comparison of the experimental and simulation temperatures for each riser as shown.

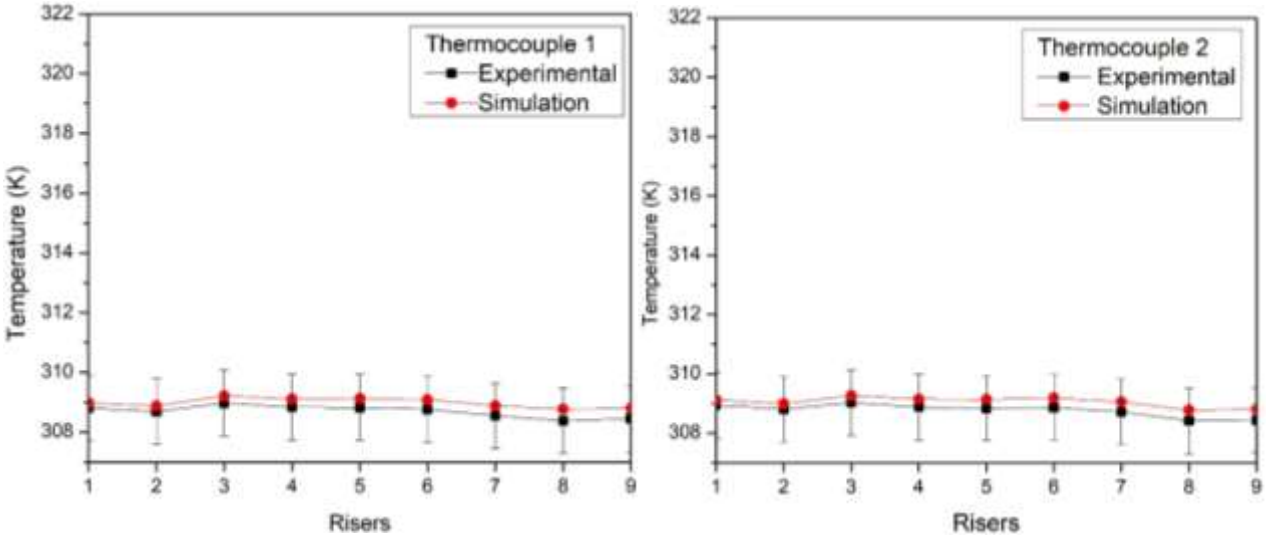

a b

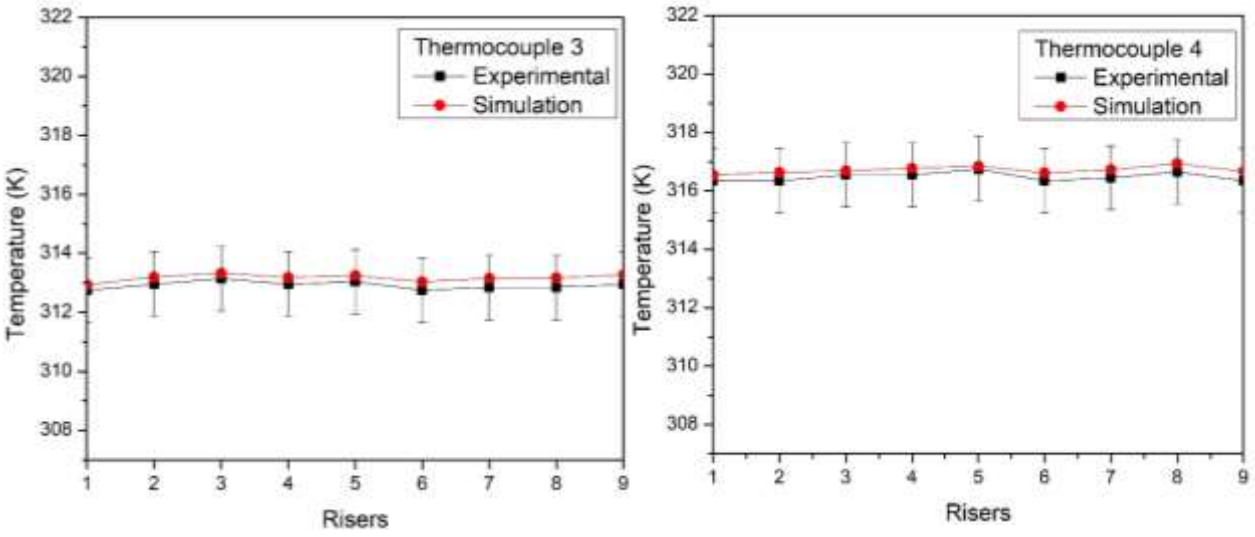

c d

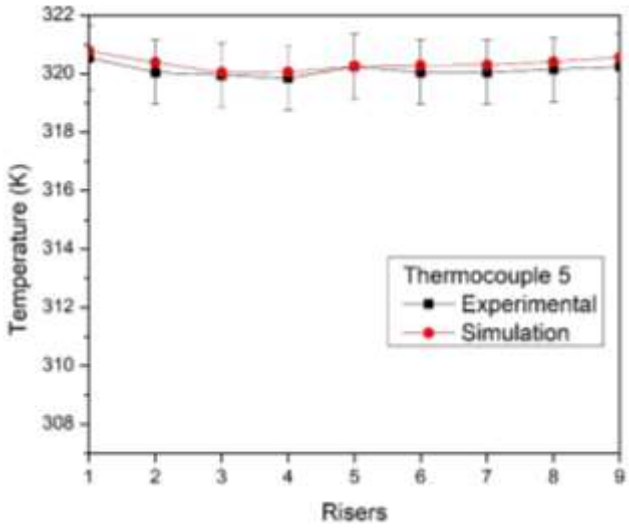

e

Figure 12. The riser's temperatures comparisons, for the case valve 25% open, are shown in the locations: thermocouples 1 (a), thermocouples 2 (b), thermocouples 3 (c), thermocouples 4 (d), and thermocouples 5 (e).

The temperatures displayed an alignment with the experimental result, as all the values are well within the error ranges of the measurements. The experimental and the simulation results of volumetric flow rate and power are listed in Table 3. The simulation heat power was used 7389.9 W and the heat loss was 254.92 W the net power in the simulation shown in the table. Additionally, the cavity inlet and outlet temperatures of the experimental and simulation results are listed in Table 3. Cavity inlet temperatures were measured from the last sub-volume

of the horizontal cold leg pipe (245), and the cavity outlet temperatures were taken after the upper manifold exit from the first sub-volume of the hot leg pipe (230).

Table 3. The total volumetric flow rate and powers results are listed for the valve 25% open.

	Experimental Results	Simulation Results
Volumetric Flow Rate (LPM)	8.2 ± 0.3	8.22
Power (Watts)	7153.12 ± 286.8	7128.98
Cavity Inlet Temperature (°C)	35.84 ± 0.2	35.93
Cavity Outlet Temperature (°C)	48.44 ± 0.2	48.64

From the simulation results, the total volumetric flow rate, cavity temperatures and power of the simulation results are also well within the error range. The model was validated for the other simulation models.

4.1.2 Normal Operation Results Case Valve 100% Open

In this model, to validate the case 100% open simulation the validated case valve 25% open model was used. The valve position was adjusted by increasing the flow area of the pipe corresponding to the valve location. The thermocouple temperatures comparison between the experimental data and the case valve 100% open results are plotted in Figure 13

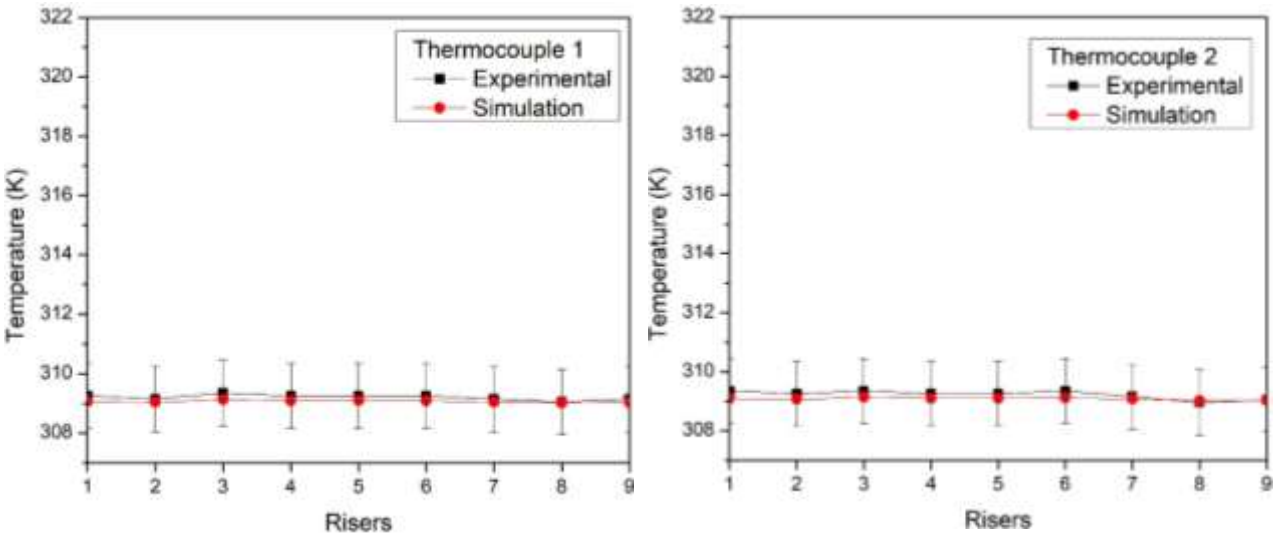

a b

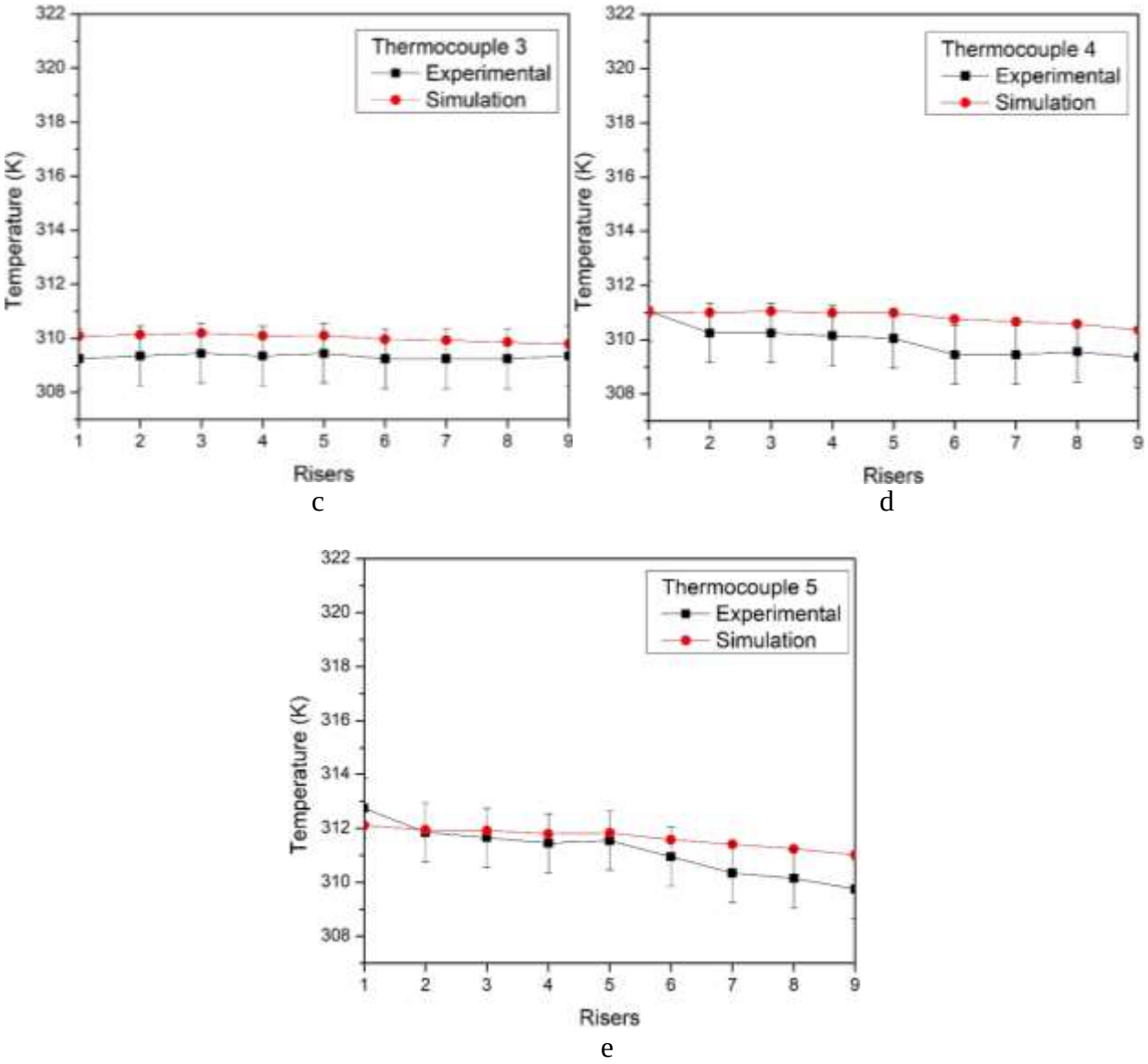

Figure 13. The risers' temperatures comparison between the case valve 100% open experimental and simulation results at locations; thermocouples 1 (a), thermocouples 2 (b), thermocouples 3 (c), thermocouples 4 (d), and thermocouples 5 (e).

The plots show that the simulated temperatures inside the risers are within the error bars of the measurement during the experiment. While the first two thermocouple temperature results showed pretty much accurate, the temperature results of thermocouples 3, 4, and 5 were acceptable. Since the cavity inlet and outlet temperatures had low error range (± 0.2 °C), high power was provided to system to reach the experimental value of cavity outlet temperature and the same heat transfer coefficients were used for both cases. The heat transfer coefficients were

adjusted for case valve 25% open and heat losses are different for both cases. Therefore, the simulation temperatures were higher than the experimental temperatures in thermocouples 3, 4, and 5 because of the heat structure and different heat losses.

The experimental and the simulation results of volumetric flow rate, power, cavity inlet and cavity outlet temperatures are listed in table 4 for the case valve fully open. In the simulation, the provided total heat power was 7866.3 W and the heat loss was 387.4 W the net power in the simulation shown in the table. Also, the cavity inlet and cavity outlet temperatures are in the error range.

Table 4. The total volumetric flow rate and powers results are listed for the valve 100% open.

	Experimental Results	Simulation Results
Volumetric Flow Rate (LPM)	39.0 ± 0.6	39.01
Power (Watts)	7555.56 ± 551.54	7478.9
Cavity Inlet Temperature (°C)	36.14 ± 0.2	35.96
Cavity Outlet Temperature (°C)	38.94 ± 0.2	38.79

From Table 4, the total volumetric flow rate and the temperatures show good agreement and the power results show an acceptable agreement. The simulation results show acceptable agreement with the experimental data.

4.2 One Riser Blockage Accident Simulation Results

In this chapter, we considered the loss of riser 4 accident results. In an RCCS facility, the loss of the riser accidents might occur for any reason hence the thermal-hydraulic behavior of the system during accident conditions is important for safety. Single riser blockage accident was simulated with RELAP5/SCDAPSIM system code to observe the system response since experiments are expensive and time-consuming. One of the central risers (riser 4) was closed

completely, and the results were observed the thermal-hydraulic behavior of the system in the accident condition. The simulation models were described in the previous chapter, two models based on the position of the valve were simulated. The data was plotted from 7000 seconds in order to analyze the system behavior after the accident. The total simulation time was set at 48000 seconds, and the data was taken every 50 seconds until the end of the simulation.

4.2.1 Case Valve 25% Open Results

The validated normal operation model case 25% open was used for this study. When the system reached the steady-state condition the trip valve located at between the riser 4 and lower manifold, was closed completely. The RELAP5/SCDAPSIM simulation results were recorded and they were plotted for investigation of the system response in this chapter.

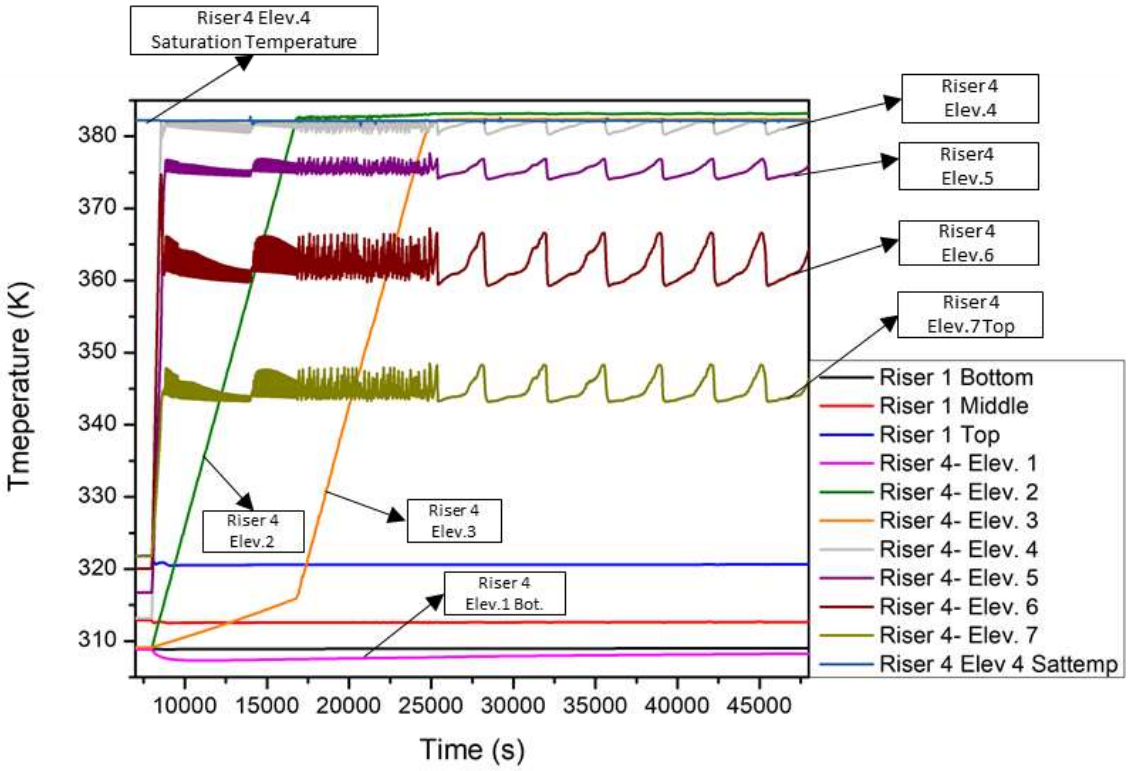

Figure 14. The liquid temperatures in the risers.

The plot in Figure 14 shows the liquid temperatures in the risers. At the blockage time (8000 seconds), the water temperature in riser 4 sharply increases, at a higher pace in sub-volumes 4, 5, 6, and 7, which correspond to the regions where more power was transferred to the coolant. Approximately 500 seconds inside the accident, the four sub-volumes on the top reached their highest temperature also the elevation 4 reached to saturation and after that time they showed oscillation in their liquid temperatures until the end of the simulation. Although the last four sub-volumes temperature results showed a sharp increase in a short time, the liquid temperatures in sub-volumes 2 and 3 (Riser 4 Elev. 2 and 3) in blocked riser showed more linear change. Since more power was transferred to the coolant from the sub-volumes 4,5, and 6 than the sub-volumes 1 and 2. The liquid temperature in sub-volume 2 increases from 305 °K to 382 °K in about 9000 seconds and the sub-volume 3 liquid temperature stabled at 382 °K about in 17000 seconds. The temperature of sub-volume 3 came to stable latest in between all sub-volumes. When the temperature of sub-volume 3 reached the upper level, the oscillations became more regular. Additionally, the temperature in sub-volume 1 did not increase as no power was given to the system at that elevation and it was connected with heat loss coming from the radiation enclosure. Therefore, the liquid temperature was cooled but not significantly because the temperature was low in sub-volume 1.

On the other hand, water temperatures in the other risers kept their steady-state condition after the closing time of the valve. The temperatures in the bottom (sub-volume 1), middle (sub-volume 4), and top (sub-volume 7) of riser 1 are shown in Figure 14. The liquid temperature in the top of the riser 1 showed a slight decrease after the accident time, the temperature in the middle sub-volume did not change and the bottom showed an insignificance rise. The

temperatures of unblocked risers were not affected as riser 4 because their heat was transferred by the coolant liquid.

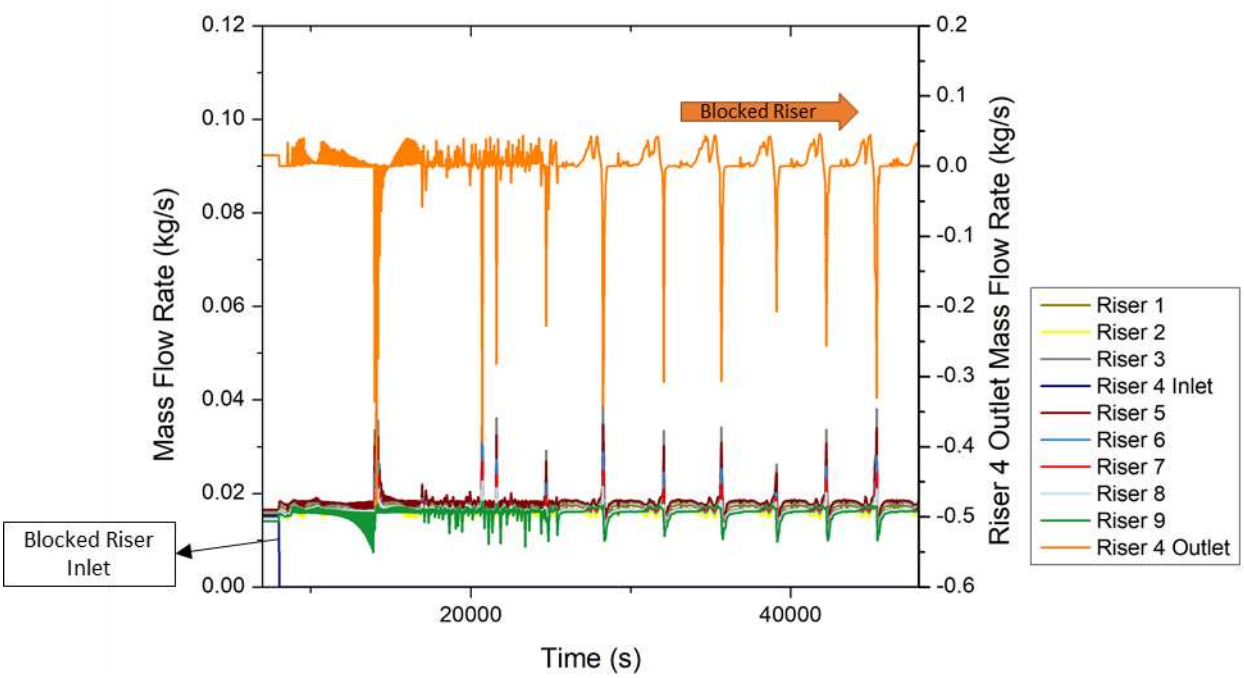

Figure 15. The mass flow rate values in the risers.

After the accident time, the water flow was blocked into riser 4, so the mass flow rate of the sub-volume 1 of riser 4 went to zero. The mass flow rate at a single junction between the sub-volume 6 and 7 were plotted in Figure 15 for risers from 1 to 9. After the blockage time, all the risers showed fluctuation in the graph. The increasing temperature causes boiling and steam production in the system, thus leading to fluctuations in the mass flow rates. The blocked riser showed mass flow rate oscillations. As the riser blocked, steam production was started with the inside the initial water in riser 4. Once the water level reached a certain level inside riser 4, the water on the top flowed into riser 4. When the peaks were positive the riser was releasing steam from the riser 4 and the negative peaks meant in the risers the fluid flows backward (from the top of the risers to the bottom). Once other risers' volumetric flow rates showed a sharp increase, the

blocked riser showed a negative sudden dramatic decrease. Then, the blocked riser took water inside at its top point because steam was generated inside riser 4 and inside water decreasing.

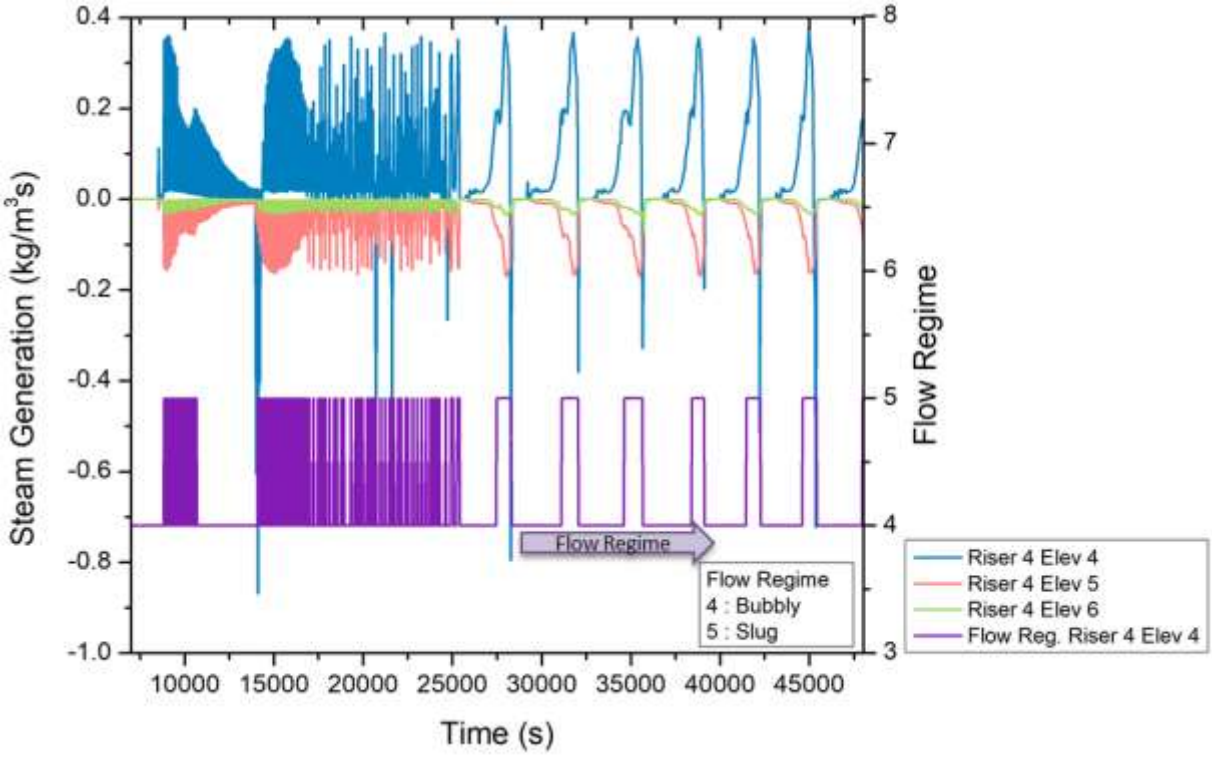

Figure 16. The steam generation and flow regime are shown.

The system produced the steam because of the high temperature in riser 4. The heat transfer was continuing to the system in riser 4 as other risers after blocking. There was fluid flow into the top of the blocked riser mentioned above, and the heat caused steam production inside the blocked riser. The steam was produced in the sub-volume 4 (Riser 4 - Elev. 4) and the generated steam was absorbed in the sub-volumes 5 and 6 (Riser 5 - Elev. 5 and Riser 6 - Elev. 6) shown in Figure 16. In the plot, the primary axis shows the steam generation and the secondary axis gives information about the flow regime of the riser 4. In the sub-volume 4 of riser 4, bubbly (4) and slug (5) flow regimes were observed. The slug flow regime was observed only in elevation 4, and in other sub-volumes of the blocked riser, only the bubbly flow regime was observed. in other sub-volumes of the blocked riser, there was only the bubbly that was

observed in the other sub-volumes of the blocked riser. The observed flow regimes in the graph were unstable and were switched faster between bubbly (4) and slug (5) after the blockage.

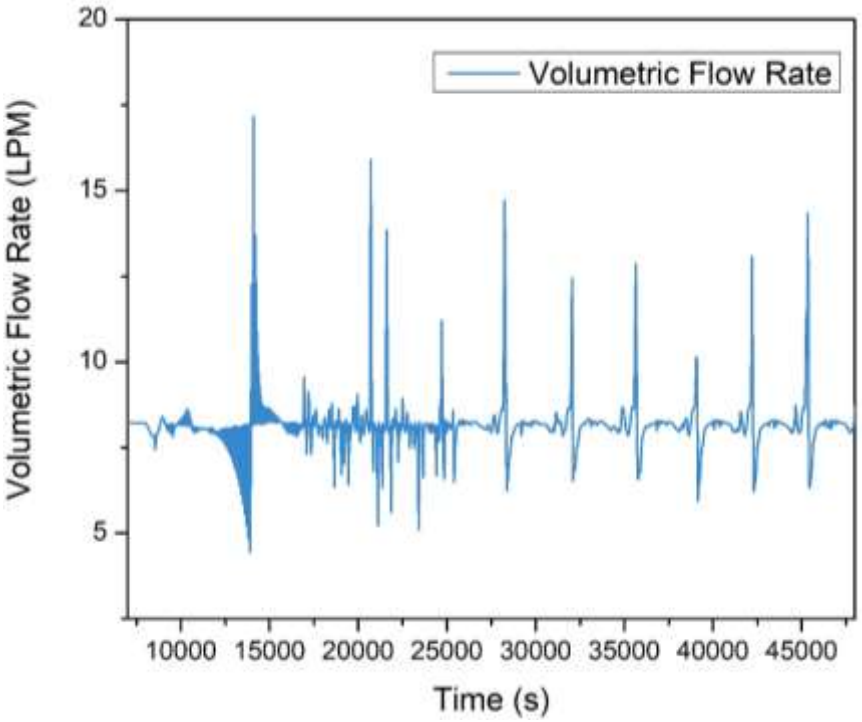

Figure 17. The system volumetric flow rate.

The system total volumetric flow rate shows fluctuation behavior around 8 LPM after the accident, the simulation volumetric flow rate results plotted in Figure 17. The temperature differences and the steam generation could cause the observed oscillations in the system.

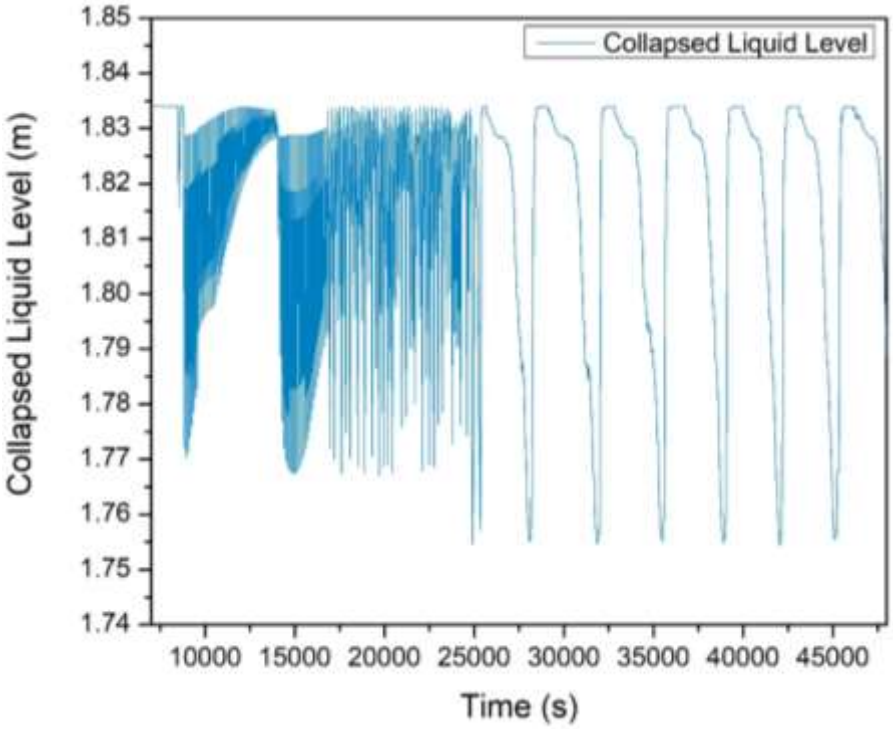

Figure 18. The collapsed liquid level in the blocked riser.

The collapsed liquid level in riser 4 (blocked riser) was plotted in Figure 18. Before the blocking, the liquid level in riser 4 was approximately 1.83 m, the water level inside riser 4 started to decrease after 8000 seconds. When the liquid level decreased below 1.76 m, the water at the top flowed inside to riser 4. The water level in the blocked riser fluctuated from the accident time until the end of the simulation due to the high temperature, and steam generation, and absorption. Once the system temperatures reached their stable values, the liquid level fluctuated more periodically.

4.2.2 Case Valve 100% Open Result

The normal operation case valve 100% open model input deck was used for this accident simulation. The accident was set at the time 8000 seconds because the system reached the steady-state condition before that time. The trip valve was located in the inlet of riser 4 and closed at 8000 seconds. The total simulation time was set to 48000 seconds to observe the

system response during one of the riser blockage accident conditions. The obtained results for this model are presented in this chapter.

The water temperatures in the risers were plotted in Figure 19. After the blockage, the liquid temperature results inside the risers were observed in a similar trend except for the blocked riser result. For this reason, only the liquid temperature of the inside riser 1 where the bottom (sub-volume 1), medium (sub-volume 4), and top (sub-volume 7) were plotted to refer to all risers except the blocked one. The liquid water temperatures in the bottom and the middle of the unblocked risers did not show any significant change after the accident as they were continuing heat transfer to the coolant. Thus, the temperatures of unblocked risers were not affected by the blocked one. It can be seen from the figure that their values show slight oscillations after the accident. The top of the unblocked risers' liquid temperature showed a slight decrease after the valve blocking after that it remained at a constant value with low oscillations.

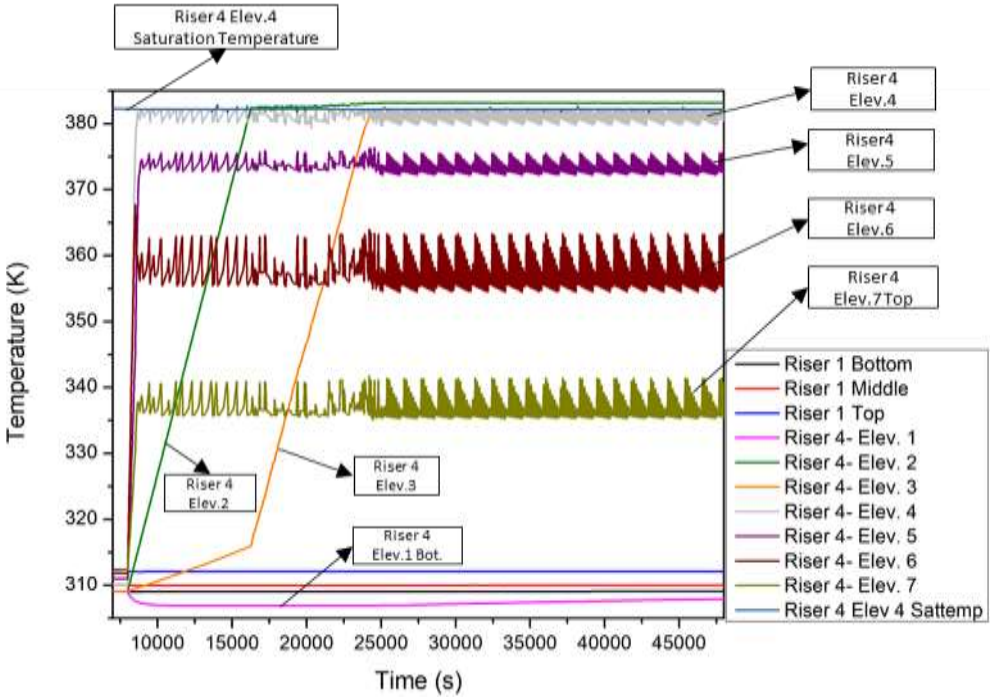

Figure 19. The liquid temperatures inside the risers.

The heat was provided to the system through the risers' sub-volumes 2 to 6 which led to the increase of temperature. In the blocked riser, liquid temperatures showed a momentary rising trend (Figure 19). Once higher temperatures levels were reached, the liquid temperatures in the sub-volumes began to fluctuate, except for the first sub-volume after 8000 seconds. After the blockage, the liquid temperature of the sub-volume 1 showed a slight decrease since there was no water flow inlet of the riser 4, no provided heat, and heat loss was added there that was coming from the radiation enclosure. Thus, the first sub-volume of riser-4 (Riser 4 - Elev. 1 - Bot.) temperature result appeared to be constant. The temperatures in sub-volumes 4, 5, 6, and 7 (Riser 4 Elev. 4, 5, 6, and 7) showed rapid incremental increases immediately and sub-volume 4 reached saturation temperature because more power was given to the coolant in these sub-volumes. The temperatures of sub-volume 2 and 3 took slightly longer to reach their highest temperature because less power was giving to the coolant from the two sub-volumes than the other sub-volumes. Once the temperature of the sub-volume 3 of the blocked riser reached to the highest temperature, the mass flow rate fluctuations became more regular and the oscillations continued until the end of the simulation.

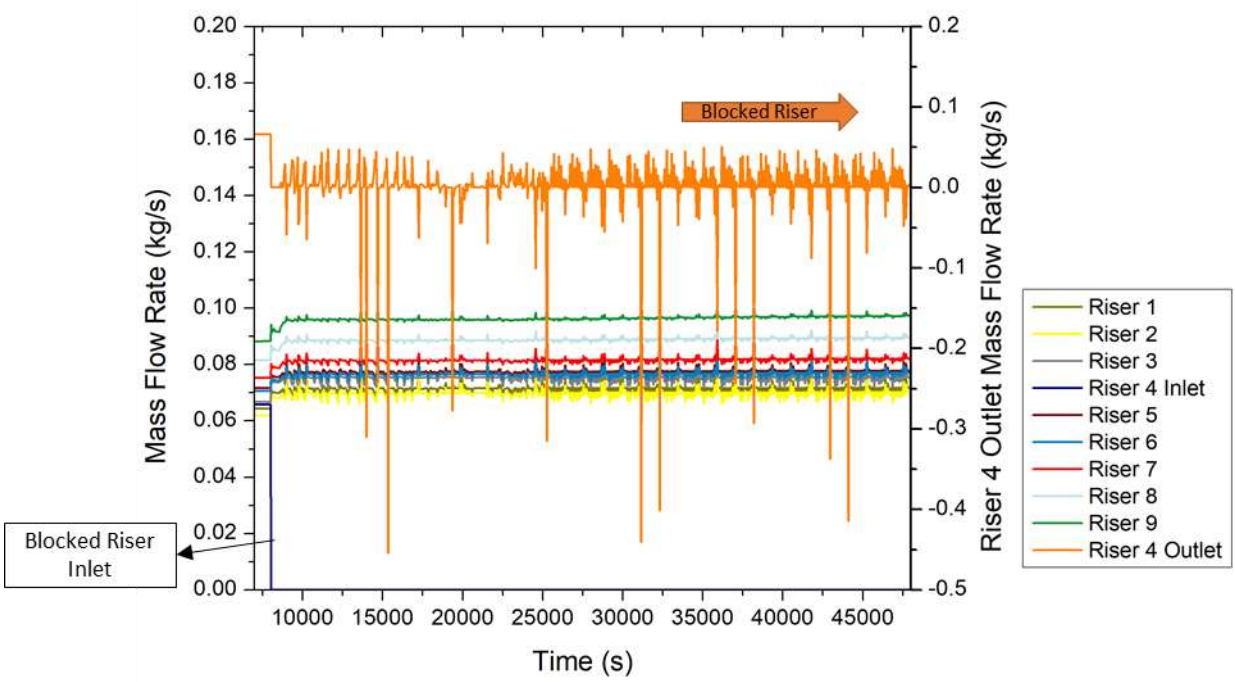

Figure 20. The mass flow rates inside the risers

The mass flow rates inside the risers were plotted in Figure 20. In the plot, the primary axis shows the single junction mass flow rate between the sub-volume 6 and 7 for all unblocked risers and the first single-junction mass flow rate of the riser 4. After the time 8000 seconds, there was no water flow to the inlet of the riser 4 (Blocked Riser Inlet) due to the blockage. Therefore, the mass flow rate of the first sub-volume of riser 4 (Blocked Riser Inlet) decreased sharply and remained zero until the end of the simulation because of the closed trip valve at the inlet of the riser 4. In the figure, all risers fluctuated after the blockage. After blockage, the increasing temperature led to boiling and vapor generation of the initial water inside the riser 4. The produced steam caused oscillations in the mass flow rates. When produced steam was releasing from riser 4, the mass flow rate of the riser 4 (blocked riser) had positive oscillations in the graph. Once the water level inside riser 4 reached a certain level, water flowed from the upper plenum to the riser interior, thereby causing negative oscillations in the mass flow rate of riser 4. All unblocked risers displayed a slight rise after the blockage time and their mass flow

rates oscillated until the end of the simulation. It can be seen in Figure 20 where unblocked risers had a sudden peak, the blocked riser had a negative peak. As riser 4 took water from the top side and the negative sign showed the direction of the flow.

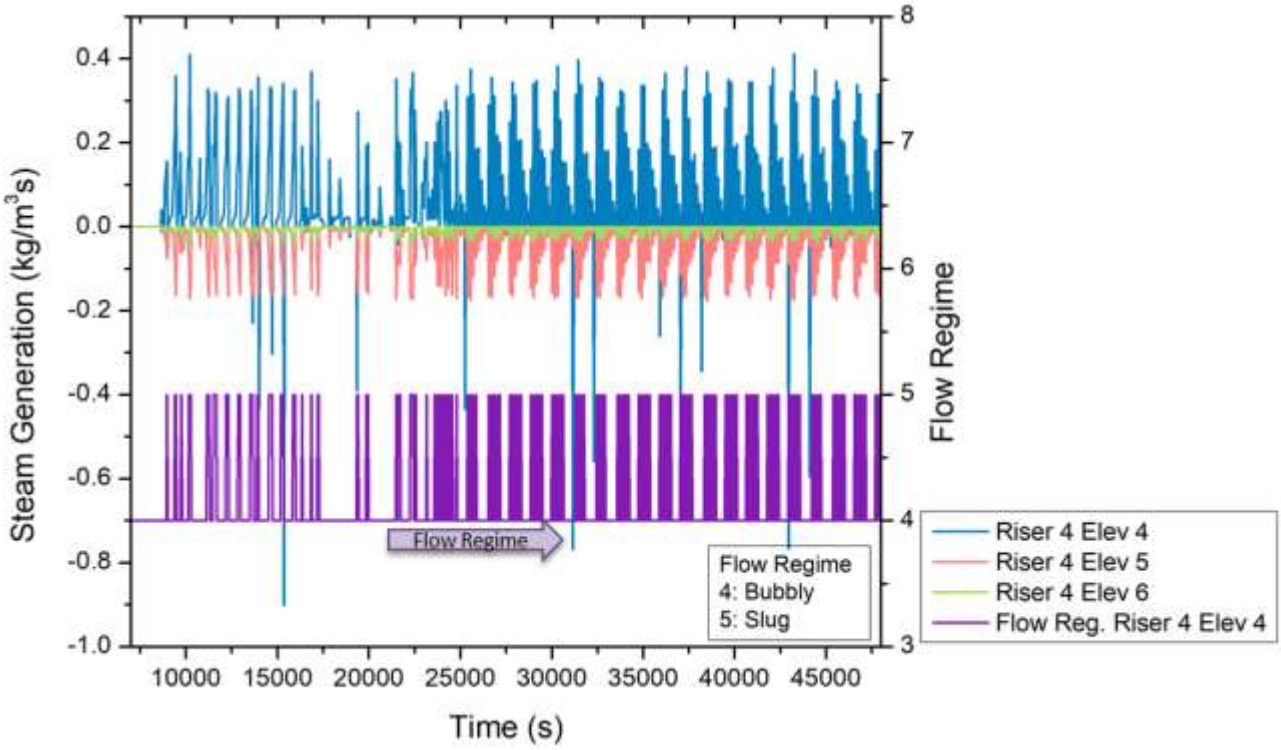

Figure 21. The steam generation and flow regime graphs.

Figure 21 shows the steam production and absorption, and the flow regimes inside the blocked riser. In riser 4, the system started to produce steam with initial water inside the riser due to increasing temperature after the accident. When the steam occurred inside the riser, the water level decreased. The vapor condensed and the riser took some water from the top of the riser to increase the water level inside the blocked riser. Therefore, the oscillations occurred during the simulation time to balance water level inside the blocked riser 4. The steam was produced in sub-volume 4 (Riser 4- Elev. 4) and condensed in sub-volumes 5 and 6 (Riser 5- Elev. 5 and Riser 6- Elev. 6). In the secondary axis, 4 refers to the bubbly flow regime and 5 refers to the slug flow

regime. The flow regimes were not stable in the system, and thus, the flow regimes bubblies and slugs were switched faster during the simulation.

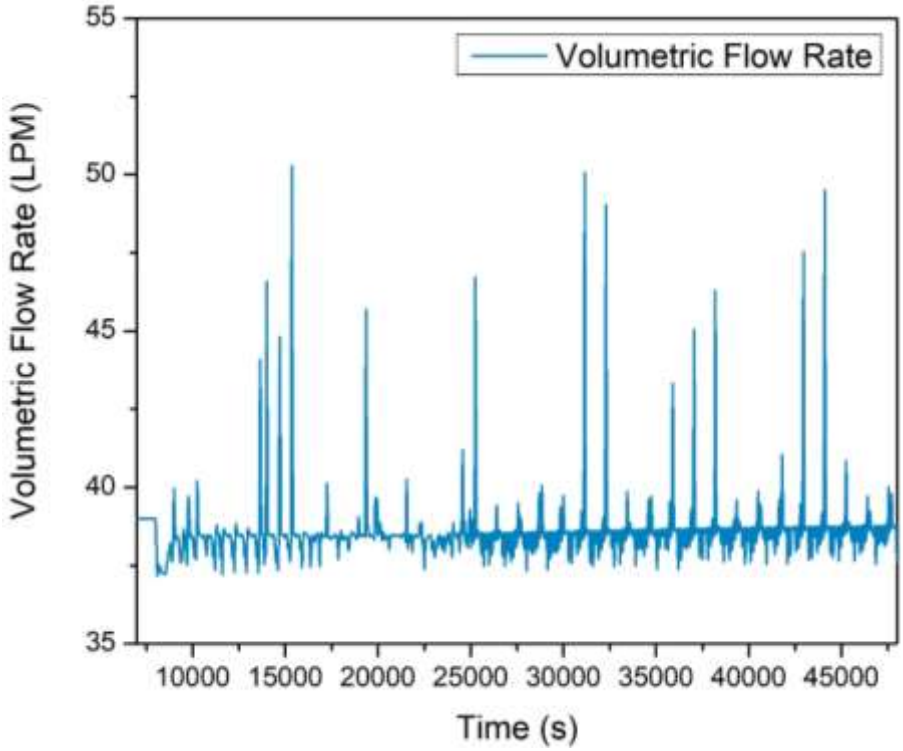

Figure 22. The total volumetric flow rate of the system.

The system volumetric flow rate was taken from the cold horizontal leg (pipe 245) where the place that volumetric flow rate data was obtained from, before the riser section and corresponding the flowmeter place in the experimental facility. The total volumetric flow rate of the system was plotted in Figure 22. After the blockage time, the volumetric flow rate of the system oscillated at around 39 LPM.

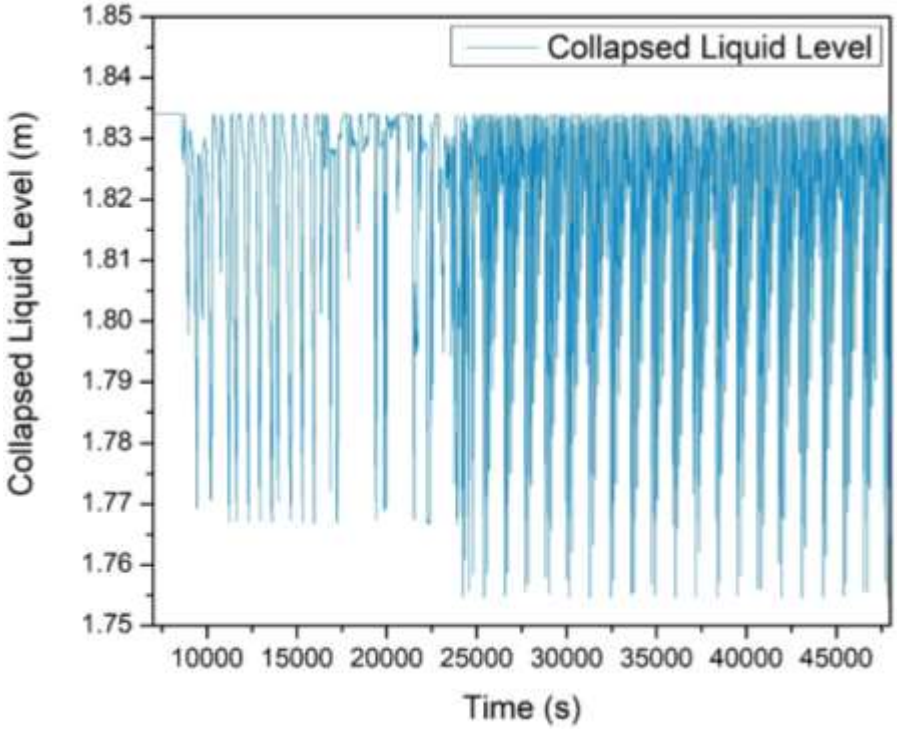

Figure 23. The collapsed liquid level in the blocked riser.

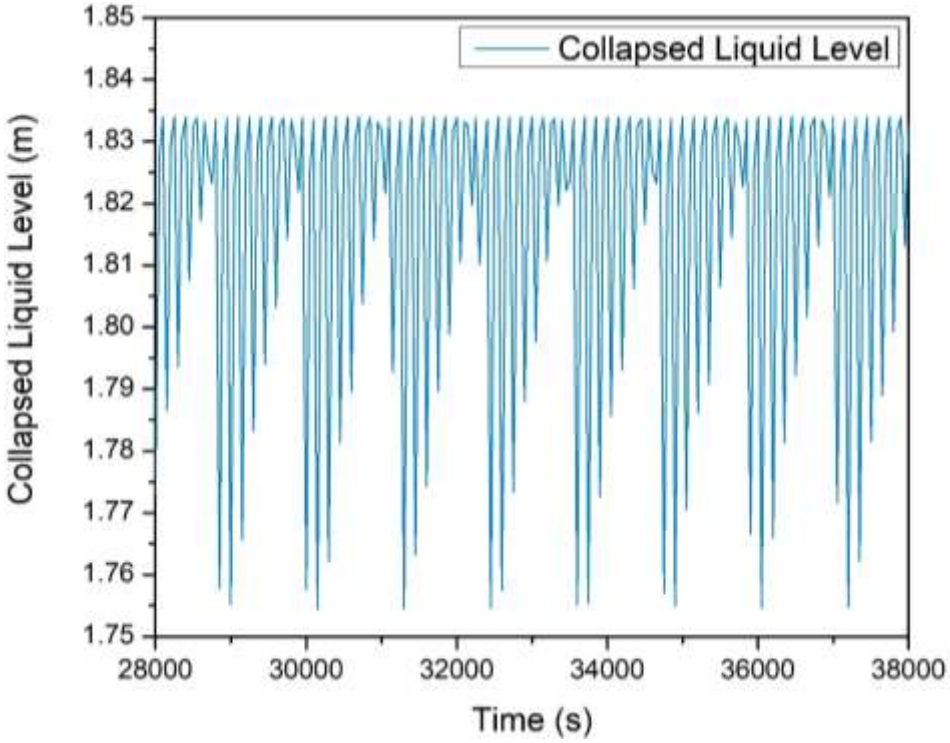

Figure 24. The collapsed liquid level oscillations in the blocked riser

The liquid level in the blocked riser (riser 4) was plotted in Figure 23. The water level before the accident was higher than 1.83 meters, and the water level started to oscillate after the

blocking. The water level of the riser 4 decreased due to the steam production in riser 4. When the liquid level inside riser 4 decreased below 1.76 meters, the water at the top flowed down and the produced vapor condensed inside riser 4. Thus, the water level increased to the initial level of approximately 1.83 m that happened many times, Figure 24. The system oscillated until the end of the simulation. When the temperatures reached stable values of about 26000 seconds, the oscillations became more regular.

4.3 Loss of the Cooling System Accident Results

In this chapter, the simulation flow characteristic and the two-phase flow instabilities were analyzed. The RELAP5/SCDAPSIM simulation model was described in chapter 3. Once the system reached the steady-state conditions (at 8000 seconds), the connection of the colling system was cut by using a trip valve (730) and a time-dependent junction (720) to observe the two-phase flow. After the accident time, the response of the natural circulation flow behavior was observed until 48000 seconds.

The simulation results of the volumetric flow rate, the cavity inlet, and exit temperature values were plotted in Figure 25. The graph started after the accident time, and it was divided into five phases based on the flow characteristic. Two-phase flow causes flow instabilities during the simulation. The cavity inlet temperature data was taken from the last sub-volume of the cold leg pipe (component 245) and the cavity outlet temperature data was taken from the first sub-volume of the hot leg pipe (component 230). The data of the system volumetric flow rate was taken in the cold leg (component 245).

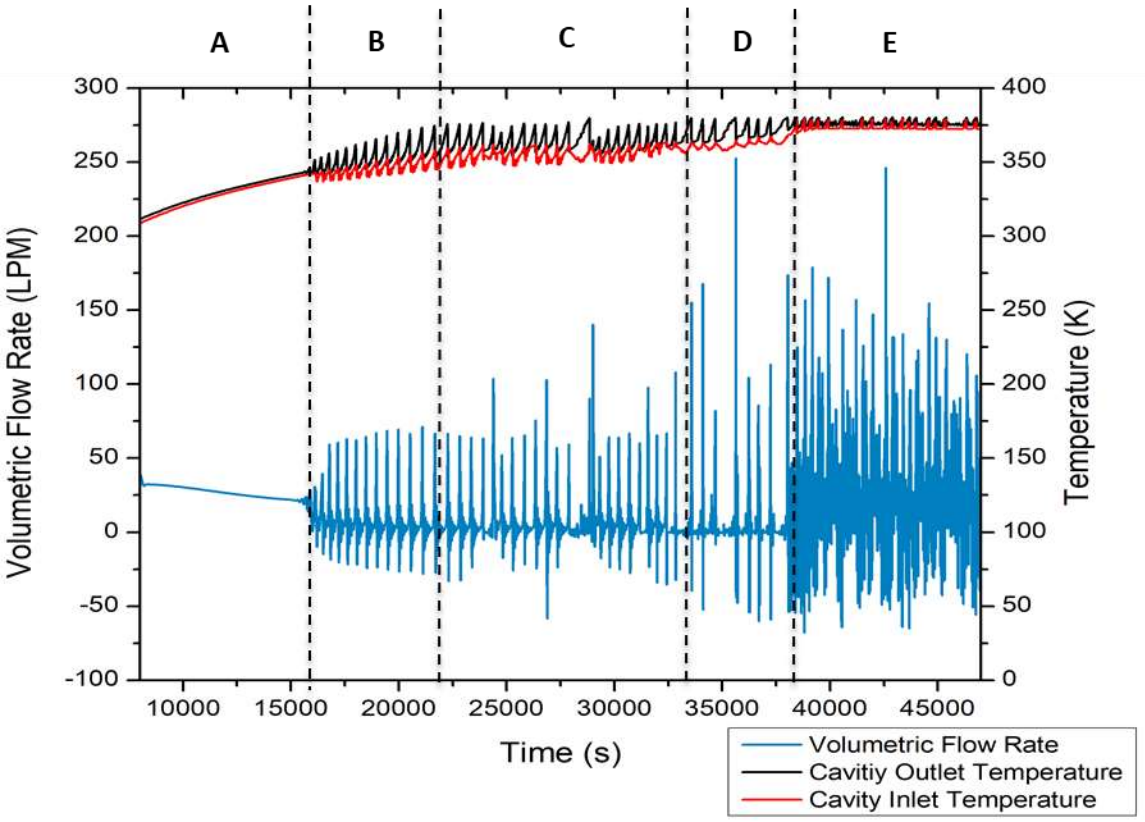

Figure 25. The total volumetric flow rate of the system, the cavity inlet and outlet temperatures are shown.

After the accident time (8000 seconds), the system showed a single-phase flow at the beginning of the accident. When the temperature of the system reached saturation, the system started to generate steam and two-phase flow was observed. From the simulation results, until 22000 seconds, only single-phase flow was observed. The first steam was generated in the vertical hot leg. The flashing instabilities are expected to observe in vertical, tall, and unheated pipes (vertical hot leg) in the systems working with natural circulation. At the exit of the heater section, the hot water experiences decrease of static pressure and subcooled, as it flows up in the vertical hot leg and reaches saturation in higher elevation of vertical riser causes the vaporization. The generated vaporization increases the driving force that causes the increase in flow rate, decrease in exit temperature, and suppression of flashing [20], [21].

Geysering expected to see in heating section. Since the high temperature, boiling started in the heating section. Bubbles occurred and expended suddenly causes vapor generation. The generated steam released from the channel and the liquid returned the subcooled condition. During the geysering process, in general, vapor eruption and condensation, and counterflow could appears. The difference of the expected instabilities are; geysering instability expected in heated sections (in risers), while in flashing instabilities are observed in tall vertical unheated sections (in Hot leg) [20], [21].

The results of the simulation data were plotted after the accident time (8000 seconds). After the cooling system was shut down, the system temperature started to increase approximately until 13000 seconds. Phase A was called between the simulation times from the beginning of the accident (8000 seconds) and 13000 seconds. In phase A, the water temperature increased and only the steady single-phase flow was observed shown in Figure 25.

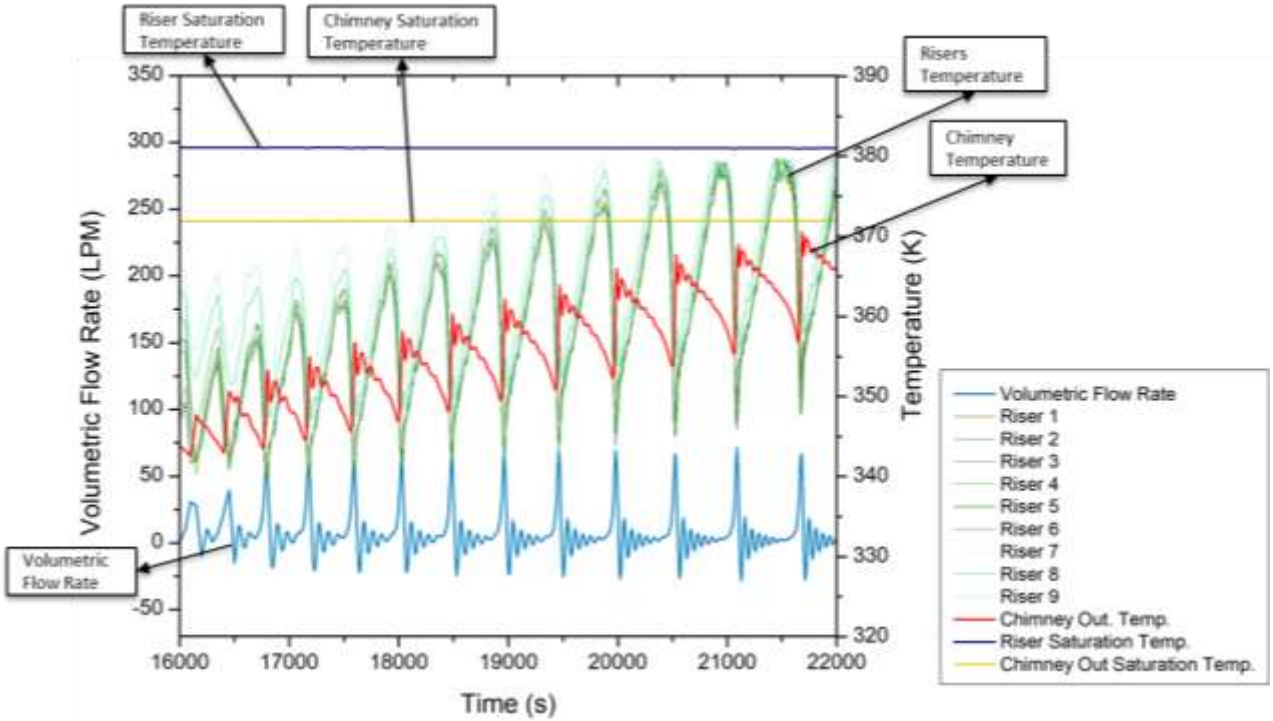

Figure 26. The phase B section flow, temperatures data and the single-phase instabilities

In phase B, the liquid temperature continued to increase. The risers exit temperatures (at the sub-volume 6, where corresponded to the thermocouple-5 place in the experiment) and the average saturation temperature of 9 risers (at the sub-volume 6 values), chimney outlet temperature in the last sub-volume of the vertical hot leg pipe (component 230) and the chimney saturation temperature at the same place plotted in Figure 26. The temperatures did not meet with their saturation temperatures in the region. Steam generation did not observe so only single-phase flow was observed in region B. In this phase, single-phase flow oscillations were observed showed in Figure 26. The average time period between the single-phase oscillations approximately 460 seconds for the phase B.

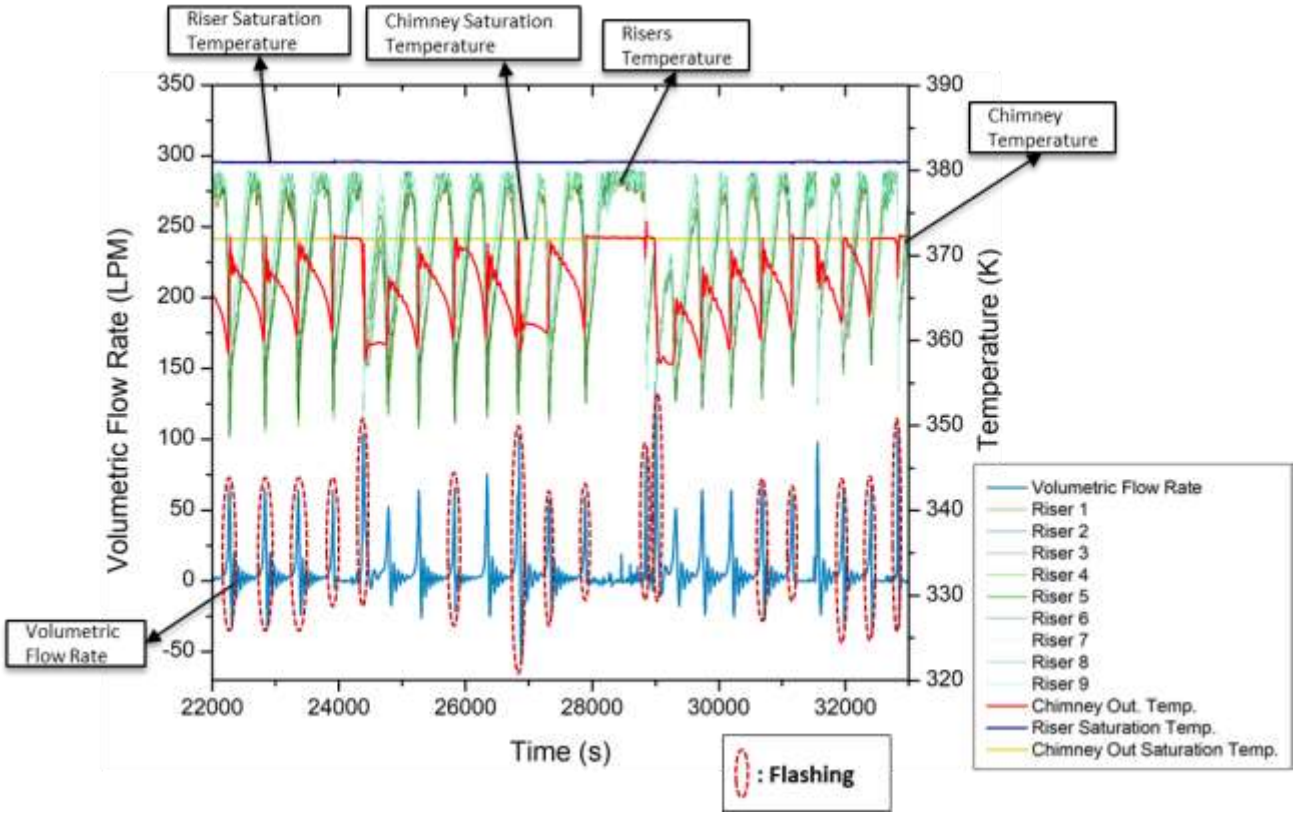

Figure 27. The phase C section flow, temperatures data and the two-phase instability flashings.

In region C, two-phase instabilities and single-phase flows were observed. When the hot fluid temperature reached saturation value, as a result, the system generated steam, and the two-phase occurred. Once the system absorbed the produced steam, the system turned to the single-phase. When the system produced and condensed vapor, this caused sudden increased and decreased peaks in temperatures and volumetric flow rate. Those peaks were two-phase instabilities and occurred in the hot leg section, Figure 27. The instabilities were called flashing since they occurred in the chimney section (in hot leg pipe 230). The hot leg component 230 was a tall and unheated pipe in the natural circulation loop. In the figure, the red dotted circles referred to the flashing instabilities. The average time period between the flashing peaks approximately 480 seconds in this phase.

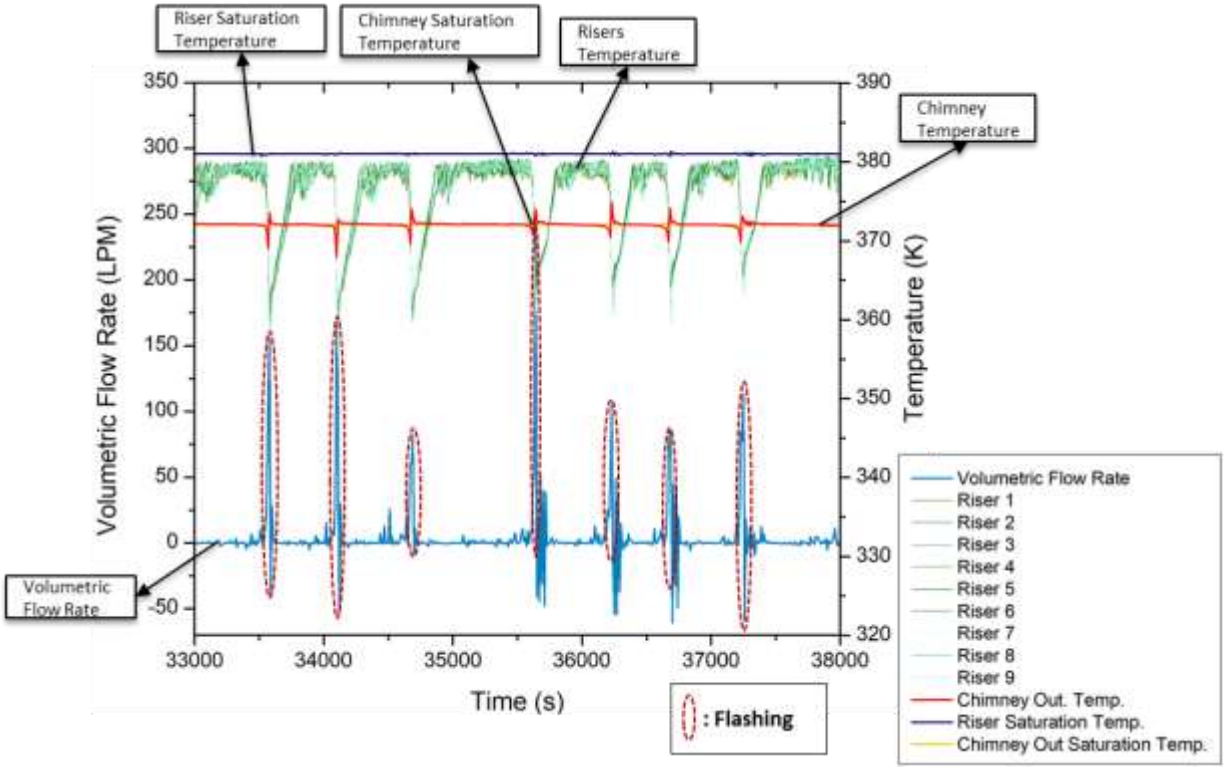

Figure 28. The phase D, the flashing instabilities and the section flow and temperatures data.

In phase D, the temperature of the chimney section reached saturation shown Figure 28. As a result, the system produced and condensed the vapor in the hot leg section. Thus, the

flashing instabilities were observed in this region as well. Additionally, the riser section temperatures increased, close to saturation value, but they had a decreasing trend when the flashing instabilities occurred. The generated vapor rose the volumetric flow rate because of the driven forces. The increased volumetric flow rate caused a decrease in temperature and condensing of flashing. The average time period between oscillations approximately 525 seconds between the flashing in phase D.

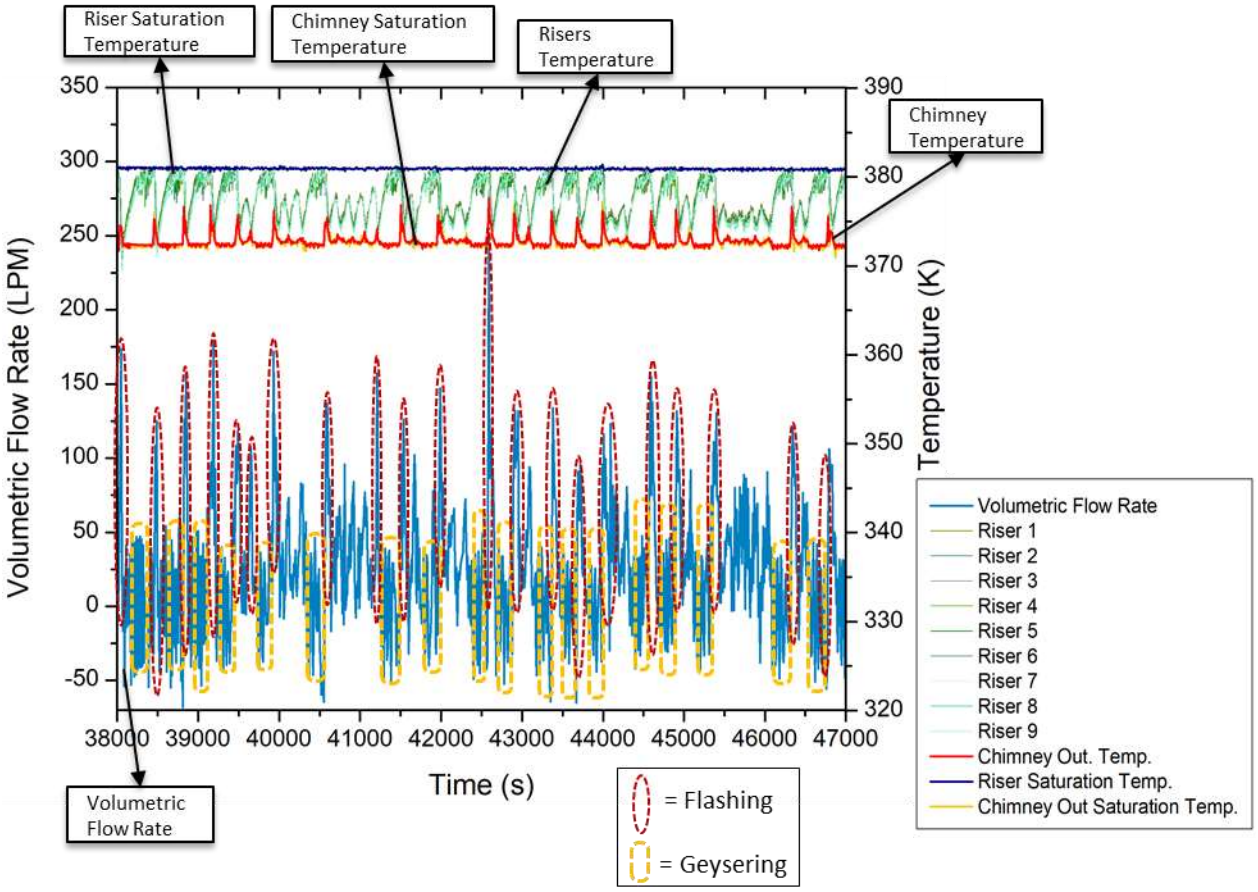

Figure 29. The phase E, the two-phase instabilities flashing and geysering, and simulation results of the system volumetric flow rate and temperatures.

In the last phase E, the system volumetric flow rate was unstable until the end of the simulation, Figure 29. The flashing instabilities were mentioned in the previous paragraph and continued in this phase. The water temperature in the riser section reached saturation, and vapor

occurred in both the riser and hot leg sections. The generated steam in the riser section caused the geysering instabilities. The black dotted rectangular shapes referred to the observed geysering instabilities in the simulation. Although the flashing instabilities had a big and single peak, the geysering had small and many peaks. The average time period between the flashing oscillations approximately 340 at the first part of the plot and 400 seconds at the last part of the graph.

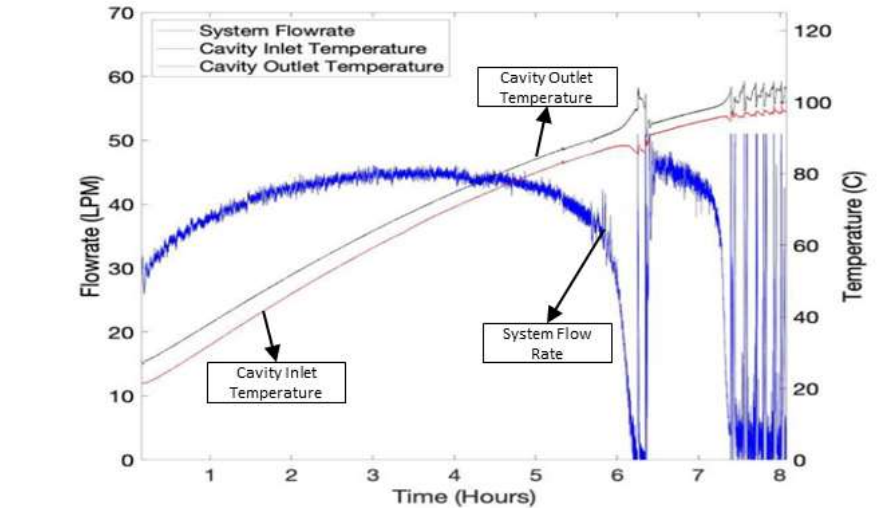

a

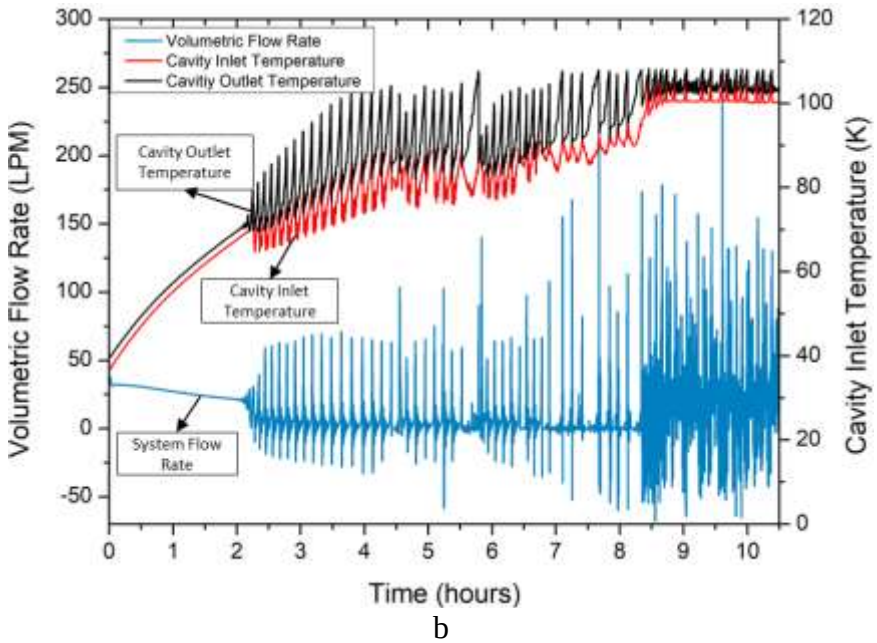

b

Figure 30. The figure on the left (a) shows the experimental results and the figure on the right (b) shows simulation results.

The cooling system loss condition was studied before for the TAMU RCCS experimental facility and the study results are represented in Figure 30a [16]. The simulation results of the loss of cooling system accident are shown in Figure 30b shows. From the figures, the temperatures increased to approximately 100 °C (saturation temperature) for both cases. The temperature profiles showed a similar trend but the simulation results had more oscillations. After reaching saturation, the two-phase flow instabilities were observed. Although only two-phase flow instability was observed in the experimental study, both single-phase and two-phase instabilities were observed in the simulation model. The flow rate results showed different trends, while the system flow rate increased time 0-2 hours after the accident in the experimental, it decreased slightly in the simulation model in 0-2 hours. After the reached saturation, stagnations were shown in the experiment and simulation. Additionally, single-phase flow instability was observed in simulation different from the experimental.

In the simulation, the same approach as the experimental study was applied to observe two-phase flow but the experimental conditions were different from the simulation. The initial conditions were different from the experimental facility. The initial conditions and heat structure could cause the differences between the two studies. When the time that cooling system was shut down, each study had different cavity temperatures. Although the cavity temperatures started at about 22°C in the experimental facility, they started from 38°C in the simulation result. Also, pressure drops might cause the differences, because we tuned our losses based on the specific range of the flow for a single-phase in static condition in the simulation model. In this study, two-phase conditions were achieved and we did not tune the heat transfer coefficient, and pressure losses for this condition. There were differences since the simulation losses might not accurate enough.

5. CONCLUSION

Reactor Cavity Cooling System normal operation simulation models were generated in RELAP5/SCDAPSIM system code-based and the Texas A&M 1/23 scaled water-cooled RCCS experimental facility. The models were case valve 25% open and case valve 100% open that depended on the valve position in the experimental facility. The simulation models were performed and validated against available experimental data. The models under normal operation conditions showed good agreement with the provided experimental data.

A second model was built to simulate the single riser blockage loss accident. The simulations showed that the single riser blockage accident in the RCCS facility would not affect its safety function and that the system would be able to remove the residual heat indefinitely even under these accident conditions.

Finally, a loss of cooling system accident was simulated for the 100% open valve case and compared with experimental data. The simulations show the rising of flow instabilities due to flashing, and geysering, that were already visible also in the experimental data, even if the model was not able to correctly predict the flow rate measured during the experiment. Moreover, the experimental and the study simulations for the loss of the cooling system scenario show an acceptable level of agreement with the experimental data for the cavity inlet and outlet coolant temperatures likely given to the fact that the power provide to the coolant is pretty much matched.

REFERENCES

[1] D. Buckthorpe, "1 - Introduction to Generation IV nuclear reactors," in *Structural Materials for Generation IV Nuclear Reactors*, P. Yvon, Ed. Woodhead Publishing, 2017, pp. 1–22.

[2] S. M. Goldberg and R. Rosner, "Nuclear Reactors: Generation to Generation," *Nucl. React.*, p. 40.

[3] M. S. El-Genk and J.-M. P. Tournier, "Reliable and safe thermal coupling of generation-IV VHTR to a hydrogen fuel production complex," *Therm. Sci. Eng. Prog.*, vol. 3, pp. 164–170, Sep. 2017, doi: 10.1016/j.tsep.2017.05.005.

[4] K. Takamatsu, "New reactor cavity cooling system (RCCS) with passive safety features: A comparative methodology between a real RCCS and a scaled-down heat-removal test facility," *Ann. Nucl. Energy*, p. 11, 2016.

[5] J. H. Song and T. W. Kim, "SEVERE ACCIDENT ISSUES RAISED BY THE FUKUSHIMA ACCIDENT AND IMPROVEMENTS SUGGESTED," *Nucl. Eng. Technol.*, vol. 46, no. 2, pp. 207–216, Apr. 2014, doi: 10.5516/NET.03.2013.079.

[6] F. Chen, Li, F., and Gougar, "Very High Temperature Reactor (VHTR) Safety Assessment," *Gen IV Int. Forum*, Jun. 2018.

[7] L. Capone, Y. A. Hassan, and R. Vaghetto, "Reactor cavity cooling system (Rccs) experimental characterization," *Nucl. Eng. Des.*, vol. 241, no. 12, pp. 4775–4782, Dec. 2011, doi: 10.1016/j.nucengdes.2011.07.043.

[8] R. Vaghetto and Y. A. Hassan, "Experimental Investigation of a Scaled Water-Cooled Reactor Cavity Cooling System," *Nucl. Technol.*, vol. 187, no. 3, pp. 282–293, Sep. 2014, doi: 10.13182/NT13-130.

[9] R. Vaghetto and Y. A. Hassan, "Modeling the thermal–hydraulic behavior of the reactor cavity cooling system using RELAP5-3D," *Ann. Nucl. Energy*, vol. 73, pp. 75–83, Nov. 2014, doi: 10.1016/j.anucene.2014.06.026.

[10] Y. Hassan, M. Corradini, A. Tokuhiro, and T. Y. C. Wei, "CFD Model Development and validation for High Temperature Gas Cooled Reactor Cavity Cooling System (RCCS) Applications," DOE/NEUP--09-817, 1159384, Jul. 2014. doi: 10.2172/1159384.

[11] N. R. Quintanar, T. Nguyen, R. Vaghetto, and Y. A. Hassan, "Natural circulation flow distribution within a multi-branch manifold," *Int. J. Heat Mass Transf.*, vol. 135, pp. 1–15, Jun. 2019, doi: 10.1016/j.ijheatmasstransfer.2019.01.102.

[12] D. Holler, R. Vaghetto, and Y. Hassan, "High-resolution wall temperature measurements with distributed fiber optic sensors," *Int. J. Therm. Sci.*, vol. 145, p. 106042, Nov. 2019, doi: 10.1016/j.ijthermalsci.2019.106042.

[13] S. J. Ball, “Next Generation Nuclear Plant Phenomena Identification and Ranking Tables (PIRTs) Volume 1: Main Report,” ORNL/TM-2007/147, 1001275, Mar. 2008. doi: 10.2172/1001275.

[14] C. Tompkins and M. Corradini, “Flow pattern transition instabilities in a natural circulation cooling facility,” *Nucl. Eng. Des.*, vol. 332, pp. 267–278, Jun. 2018, doi: 10.1016/j.nucengdes.2018.03.018.

[15] J. A. Boure, A. E. Bergles, and L. S. Tong, “Review of two-phase flow instability,” *Nucl. Eng. Des.*, vol. 25, no. 2, pp. 165–192, Jul. 1973, doi: 10.1016/0029-5493(73)90043-5.

[16] R. Vaghetto, S. Yang, D. Hodge, and Y. Hassan, “Two-phase flow measurements and observations in a cooling panel of the reactor cavity cooling system,” *Prog. Nucl. Energy*, p. 103578, Dec. 2020, doi: 10.1016/j.pnucene.2020.103578.

[17] “NRC: SCDAP/RELAP5/MOD 3.3 Code Manual (NUREG/CR-6150),” May 1988, Accessed: Nov. 20, 2020. [Online]. Available: https://www.nrc.gov/reading-rm/doc-collections/nuregs/contract/cr6150/.

[18] C. M. Allison and J. K. Hohorst, “Role of RELAP/SCDAPSIM in Nuclear Safety,” *Science and Technology of Nuclear Installations*, Apr. 13, 2010. https://www.hindawi.com/journals/stni/2010/425658/ (accessed Nov. 13, 2020).

[19] S. Šadek, “ISP-46 Analysis with RELAP5/SCDAPSIM Computer Code,” p. 13, 2003.

[20] A. K. Nayak and P. K. Vijayan, “Flow Instabilities in Boiling Two-Phase Natural Circulation Systems: A Review,” *Sci. Technol. Nucl. Install.*, vol. 2008, pp. 1–15, 2008, doi: 10.1155/2008/573192.

[21] X. Yan, G. Fan, and Z. Sun, “Study on flow characteristics in an open two-phase natural circulation loop,” *Ann. Nucl. Energy*, vol. 104, pp. 291–300, Jun. 2017, doi: 10.1016/j.anucene.2016.12.038.